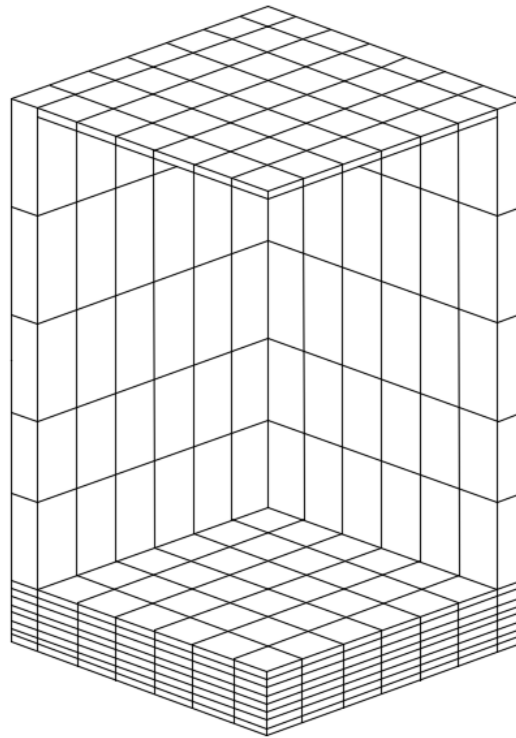




**CHALMERS**  
UNIVERSITY OF TECHNOLOGY

---



# Dynamic process of steam in a super critical CFB boiler

Master's thesis in Master Programme Innovative and Sustainable Chemical Engineering

Ivana Staničić



MASTER'S THESIS 2018:SEEX30

# Dynamic process of steam in a super critical CFB boiler

Ivana STANIČIĆ



**CHALMERS**  
UNIVERSITY OF TECHNOLOGY

Department of Space, Earth and Environment  
*Division of Energy Technology*  
CHALMERS UNIVERSITY OF TECHNOLOGY  
Gothenburg, Sweden 2018

Dynamic process of steam in a super critical CFB boiler

Ivana STANIČIĆ

© Ivana STANIČIĆ, 2018.

Examiner: Assoc. Prof. David PALLARÈS, Chalmers University of Technology, Department of Space, Earth and Environment

Supervisor: Prof. Dr. Hairui YANG, Tsinghua University, Department of Energy and Power Engineering

Master's Thesis 2018:SEEX30

Department of Space, Earth and Environment

Energy Technology

Chalmers University of Technology

SE-412 96 Gothenburg

Telephone +46 31 772 1000

Cover: Visualisation of the mesh of a simplified 350 MW CFB boiler [1].

Typeset in L<sup>A</sup>T<sub>E</sub>X

Gothenburg, Sweden 2018

Dynamic process of steam in a super critical CFB boiler

Ivana STANIČIĆ

Department of Space, Earth and Environment

Chalmers University of Technology

## Abstract

CFB technology has gained more attention over the past few years. Most probably due to its efficiency and ability of achieving low emissions. New strict governmental regulations regarding emissions are continuously imposed which makes CFB boilers a promising candidate for future industries. One way to facilitate the implementation of CFB boilers is by making it cheap option. Currently these boilers are equipped with expensive urgent feed water systems for boiler safety, in case of electricity loss. Since there are no accident records this equipment is still in controversy.

This thesis analyses the physical process of steam in a 350 MW super critical circulating fluidized bed boiler during sudden electricity failure. By obtaining information about the dynamic process of steam properties it will be possible to estimate the necessity of the urgent water feeding system in future applications.

With some simplifications a three dimensional model was created to solve energy equations. The model includes thermal processes like conduction, radiation and convection of steam, bulk material and air. The final model predicts the dynamic progress of these.

The highest temperatures achieved is located in the bottom of the furnace, the conductive part, and lies around 875 K which is slowly continuing to increase. However, this temperature lies in the acceptable span for wall conditions which indicates a possibility for economic savings. Further studies need to be conducted in order to conclude whether the emergency system can be neglected.

Keywords: super critical steam, circulating fluidizing bed boiler, electricity failure, safety



## *Acknowledgements*

First I would like to thank my examiner Assoc. Prof. David PALLARÈS at Chalmers University of Technology and my supervisor Prof. Dr. Hairui YANG at Tsinghua University. Whenever I ran into a trouble spot or had a question about my research or writing they always welcomed me. They consistently allowed this paper to be my own but steered me into the right direction whenever I needed it.

I would also like to acknowledge Assoc. Prof. Henrik LEION for his time and effort. Without his valuable help and guidance the exchange with Tsinghua University would not be possible and this thesis would not exist.

I am particularly grateful for the assistance given by the CFB research group at Tsinghua University. Without their enthusiastic contribution and input, the research could not have been successfully conducted.

I am utterly thankful for the scholarships I have recieved; ÅF Resestipendium, Anna Whitlocks Minnesfond and Estrid Ericsons Stiftelse. Without their contribution the exchange with Tsinghua would not be possible.

I would like to thank Karolina LJUNGBERG at Luleå University of Technology for her effort and artistic skills that helped me with proper figures and made the overall impression professional.

I would also like to acknowledge Viktor ANDERSSON and Christoffer SELLGREN at Chalmers University of Technology as the second readers, and I am gratefully indebted to them for their very valuable comments on this thesis.

Finally, I must express my very profound gratitude to Amer MESIC and my family for providing me with unfailing support and continuous encouragement throughout my years of study and through the process of researching and writing this thesis. This accomplishment would not have been possible without them.

Thank you,

Ivana STANIČIĆ

# Contents

<b>Introduction</b>	<b>1</b>
1 Objective . . . . .	1
2 Scope . . . . .	1
3 Constraints . . . . .	1
4 Background . . . . .	2
<b>Theory</b>	<b>4</b>
5 Heat transfer mechanisms . . . . .	4
5.1 Convection . . . . .	4
5.2 Thermal conduction . . . . .	4
5.3 Radiation . . . . .	4
6 Finite Volume Method . . . . .	5
6.1 Discretization schemes . . . . .	6
6.2 Explicit and implicit schemes . . . . .	6
7 Energy balance . . . . .	7
<b>Method</b>	<b>9</b>
8 Geometrical description . . . . .	9
9 Energy equation for solids . . . . .	10
9.1 Discretization schemes . . . . .	10
9.2 Boundary conditions . . . . .	10
10 Energy equation for air . . . . .	11
11 Energy equation for steam . . . . .	11
12 Initial conditions . . . . .	12
13 Code structure . . . . .	14
<b>Results and discussion</b>	<b>15</b>
14 Dynamic solid progress . . . . .	16
15 Dynamic steam progress . . . . .	17
16 Simulation process . . . . .	21
17 Future work . . . . .	21
<b>Conclusions</b>	<b>23</b>
<b>Bibliography</b>	<b>24</b>



# List of Figures

1	Schematic figure of a CFB boiler [8]. . . . .	2
2	Schematic figure of emergency water supply system [10]. . . . .	3
3	Two elemental areas in arbitrary configuration where $i=1$ and $j=2$ . Arrows are normal vectors to respective surface. . . . .	5
4	Illustration of labels for nodes [15]. . . . .	6
5	A fluid element [15]. . . . .	7
6	Simplified geometry and mesh of furnace [1]. . . . .	9
7	Initial profiles for one vertical wall. . . . .	13
8	Temperature profile for air. . . . .	15
9	Temperature profile for solids. . . . .	16
10	Temperature profile in south steam wall. . . . .	18
11	Conductive area after 200 seconds. . . . .	19
12	Radiating area after 200 seconds. . . . .	19
13	Heat transferred through south steam wall. . . . .	20
14	Dimensions of two perpendicular rectangular surfaces [13]. . . . .	iii
15	Dimensions of two parallel rectangular surfaces [13]. . . . .	iv
16	Description of MatLab functions, main file and database, part 1. . . . .	vi
17	Description of MatLab functions, main file and database, part 2. . . . .	vii
18	Description of MatLab functions, main file and database, part 3. . . . .	vii
19	Temperature profile after 30 seconds. . . . .	ix
20	Temperature profile after 60 seconds. . . . .	x
21	Temperature profile after 100 seconds. . . . .	x
22	Temperature profile after 200 seconds. . . . .	xi
23	Temperature profile after 30 seconds. . . . .	xii
24	Temperature profile after 60 seconds. . . . .	xii
25	Temperature profile after 100 seconds. . . . .	xiii
26	Temperature profile after 200 seconds. . . . .	xiii

# List of Tables

1	Initial conditions. . . . .	12
2	Values of constants. . . . .	13
3	Properties for wall, air, steam, sand and bed material. . . . .	14
4	Placement of temperature 1D profiles. . . . .	17

# List of Abbreviations

<b>CFB</b>	<b>Circulating Fluidized Bed</b>
<b>CV</b>	<b>Control Volume</b>
<b>DFB</b>	<b>DongFang Boiler</b>
<b>FVM</b>	<b>Finite Volume Method</b>
<b>PCV</b>	<b>Pressure Control Valve</b>

# Physical Constants

Stefan Boltzmann's constant	$\sigma = 5.670\,40 \times 10^{-8} \text{ W m}^{-2} \text{ K}^{-4}$
Gravity of earth	$g = 9.81 \text{ m s}^{-2}$
Gas constant	$R = 8.3145 \text{ J mol}^{-1} \text{ K}$
Individual gas constant for air	$R/M_{gas} = 287.05 \text{ J kg}^{-1} \text{ K}$

# List of Symbols

$A$	area	$\text{m}^2$
$c_p$	heat capacity	$\text{J kg}^{-1} \text{K}^{-1}$
$d_w$	wall thickness	$\text{m}$
$d_t$	tube diameter	$\text{m}$
$F_{ij}$	view factor	-
$h$	heat transfer coefficient	$\text{W m}^{-2} \text{K}^{-1}$
$k$	heat conductivity	$\text{W m}^{-1} \text{K}^{-1}$
$N$	number of surfaces	-
$P$	pressure	$\text{Pa}$
$p$	number of segments	-
$Q$	accumulated energy in one solid CV	$\text{W}$
$q$	energy	$\text{W}$
$\dot{q}$	energy flux	$\text{W m}^{-2}$
$R$	thermal resistance	$\text{K W}^{-1}$
$S$	source term	$\text{W}$
$s$	distance between two surface elements	$\text{m}$
$T$	temperature	$\text{K}$
$V$	volume	$\text{m}^3$
$x$	width of element	$\text{m}$
$y$	length of element	$\text{m}$
$z$	height of element	$\text{m}$
$\varepsilon$	emissivity	-
$\theta$	angle	$\text{rad}$
$\rho$	density	$\text{kg m}^{-3}$
$\Phi$	any property	-

# Introduction

As a result of the economic development, the world's energy requirements are growing. Statistics show that this growth can be observed in the increasing consumption of coal, oil and other fuels [2]. This has, and will continue to have negative environmental effects. However, new energy efficient technologies have become popular fields of research. Amongst these relatively new technologies are the circulating fluidized bed (CFB) boilers. CFB technology has gained more attention over the past years. Most probably due to its efficiency and ability of achieving low emissions. New strict governmental regulations regarding emissions are continuously imposed, which makes CFB boiler a promising candidate for future industries [3]. CFB boilers are fuel efficient and there are even possibilities to implement carbon capturing techniques which enables low carbon dioxide emissions [4]. By combusting biofuel even negative emissions may be achieved and carbon dioxide removed from the atmosphere [5].

One way to facilitate the implementation of CFB boilers in industries is to make it economically viable. Currently CFB boilers are equipped with urgent water feeding system for boiler safety during electricity loss. This type of equipment has an investment cost around 27 million SEK [6], excluding extra cost for regular safety checks. For a 350 MW boiler it is estimated that the total loss of a single electricity failure accident is around 14 million SEK [6]. The most critical event for the water feeding system would be in case of electricity loss. There are currently no field test data, accident records or previous studies regarding this subject. Therefore the water feeding system is still in controversy.

## 1 Objective

The purpose of this thesis is to investigate the dynamic change of steam temperature in a super critical CFB boiler during electricity loss in order to conclude whether economic savings can be made or not.

## 2 Scope

The thesis will cover boiler sizes of 350 MW and only of the type super critical CFB. The geometry is simplified which excludes furnaces with wing walls, division walls and refractory. Also corrosion on tubes has been neglected. However the produced code is general and by changing initial conditions ultra super critical steam and larger boilers can be simulated.

## 3 Constraints

Considering time limitations and available computer power only energy balances will be solved. In order to make an efficient program the boiler has been simplified

to a quadrangular form and assumptions for developed heat equations are discussed further on.

## 4 Background

Combustion in CFB boilers occur at relatively low temperature which regulates the production of nitrogen oxides and minimizes fouling and slagging. Another advantage with these type of boilers is the possibility to use a wide range of fuels [7]. A typical setup of CFB boilers is illustrated in figure 1. Depending on the manufacturer the design might be somewhat different, however the basic principles remain the same.

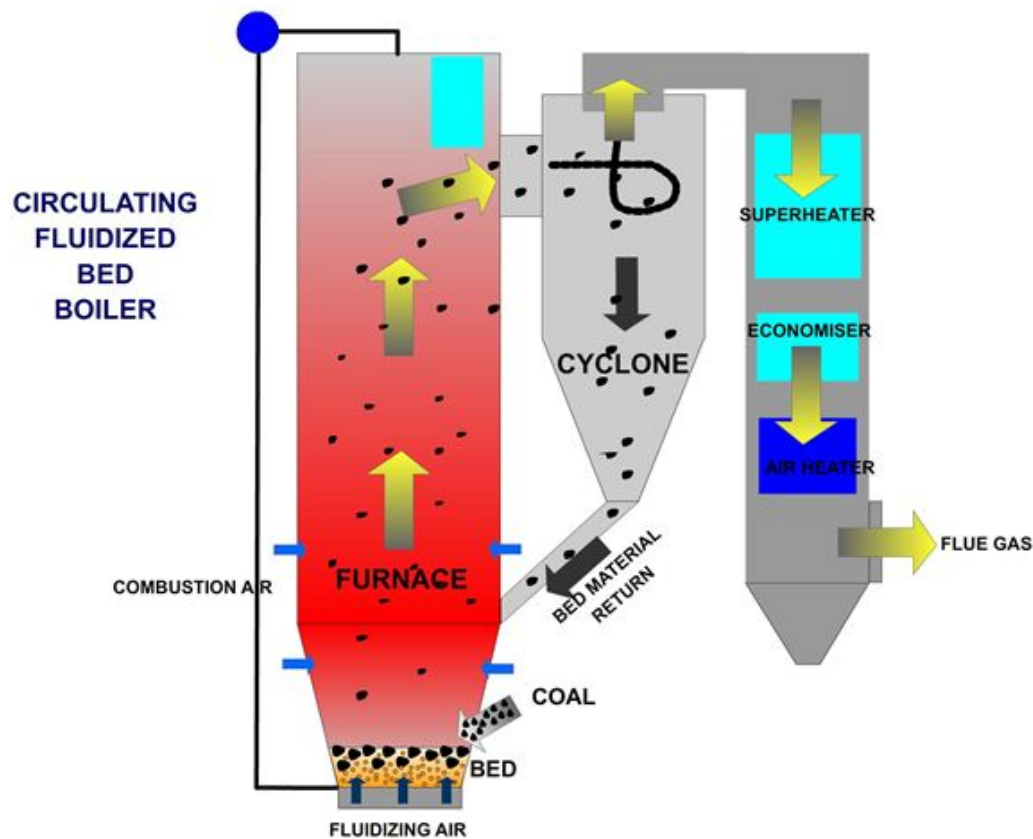


FIGURE 1: Schematic figure of a CFB boiler [8].

At the bottom of the boiler is a bed of inert material, mostly some sort of sand, which is mixed with fuel. Limestone may be added in order to reduce the sulphur oxide emissions if sulphur rich fuels are used. Air is supplied by a drive fan at high pressure which lifts the bed material and keeps it in suspension. At this stage combustion occurs. Air is supplied at several levels for an even distribution. Particles of coal, ash and bed material are carried along with flue gases into the cyclone where the heavier

particles are separated and brought back to the bed. The remaining hot gases from the cyclone pass heat transfer surfaces and exit the boiler. When CFB boilers operate at steady state the heat released from the combustion will be adsorbed by the steam in the heating surfaces surrounding the furnace. Therefore the furnace and steam temperature will be constant and stable.

CFB boilers contain around hundred tons of circulating high temperature bed material which may lead to danger during electricity loss. After power outage the water feeding pump will shut off causing a breakdown of water supply. Simultaneously all air fans, draft fan and fuel supply will stop. Bed material will drop to the bottom and accumulate continuing to release heat to surrounding surfaces.

Since the super critical CFB bed does not have a steam drum the feed water goes straight from the boiler furnace to the steam turbine. In case of electricity loss the feed water pump will stop and no more feed water will enter the tubes. Thereafter the emergency pressure releasing valves will automatically open and the high pressure steam released into the atmosphere [9]. Steam in heating surface tubes will decrease and the temperature and pressure of the steam change dynamically.

There are several possible outcomes of this event. If the radiated heat from the accumulated hot solids in the bottom can not be adsorbed by the steam, the wall temperature will increase until it reaches a point when the tubes will burst. This could pose a risk to structural integrity and/or explosion hazards. For a 350 MW super critical CFB boiler the total loss of such an event may be estimated to over 14 million SEK. To reduce these losses some boilers are equipped with an emergency water supply system. The initial investment cost for such a set is estimated to around 27 million SEK, excluding additional costs for regular safety checks, see figure 2 for illustration.

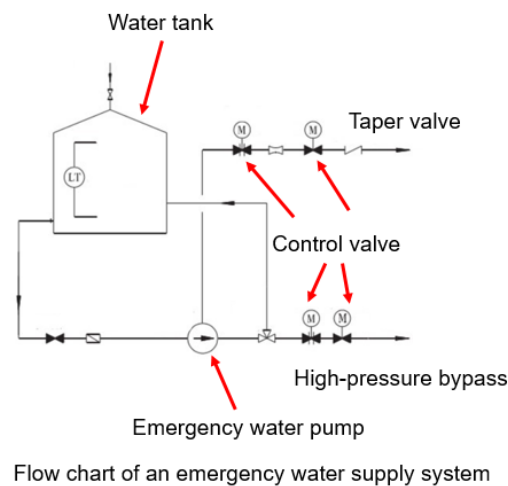


FIGURE 2: Schematic figure of emergency water supply system [10].

There are currently no field test data, accident records or previous studies regarding this subject. Electricity loss is a small probable event and urgent water feeding system is relative expensive. If the walls do not reach the temperature limitation these costs might be saved [9]. Due to these high costs and lack of data the requirement for an urgent water feeding system for boiler safety is still in controversy.



# Theory

This chapter gives an introduction to the heat transfer concept and mechanisms relevant to this thesis in order to strengthen the calculations and assumptions.

## 5 Heat transfer mechanisms

Energy can be transferred through many different ways. The most general way of describing the energy equation is by the following terms

$$''Accumulation = Input - Output + Source''$$

Below are some relevant mechanisms in which these terms can be expressed. Their mathematical descriptions are explained further.

### 5.1 Convection

Convection is comprised of two mechanisms. Besides energy transfer due to diffusion it can also be transferred by bulk motion. If a temperature gradient is present this would result in heat transfer [11]. There are several types, forced and natural convection. Forced convection occurs due to flow caused by external means while the latter occurs due to buoyancy forces. Convection is quantified with the convection heat transfer coefficient  $h$ , unique for each fluid and circumstance. Equation 1 shows the mathematical description.

$$q = hA(T - T_{inf}) \quad (1)$$

Here  $T$  is the surface temperature,  $T_{inf}$  fluid temperature and  $A$  heat transfer area.

### 5.2 Thermal conduction

The law of conduction, also known as Fourier's law [12], shows that the heat flux depends on the material conductivity,  $k$  and temperature gradient, see equation 2 for the complete 3D case.

$$q = -kA\nabla T \quad (2)$$

### 5.3 Radiation

Another heat transfer mechanism is thermal radiation. This type of electromagnetic radiation is generated by thermal motion of all particles. Consequently all materials with a temperature above absolute zero will emit radiation. However it may not be a major contribution at lower temperatures. The mathematical description of this process is presented in equation 3.

$$q_{i \rightarrow j} = \varepsilon \sigma A F_{i \rightarrow j} (T_i^4 - T_j^4) \quad (3)$$

Equation 3 describes the radiated energy of a grey body per unit time from area  $i$  to area  $j$ . Here  $\sigma$  is the Stefan-Boltzmann constant,  $\varepsilon$  is the emissivity factor and  $A$  the radiating surface area. One term which will require more attention is the view factor  $F_{i \rightarrow j}$ . The most general form for the view factor can be seen in equation 4 [11].

$$F_{i \rightarrow j} = \frac{1}{A_i} \int_{A_i} \int_{A_j} \frac{\cos(\theta_i) \cos(\theta_j)}{\pi s^2} dA_j dA_i \quad (4)$$

Definition of angles and areas is illustrated in figure 3.

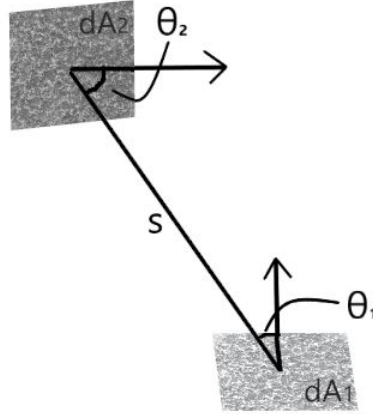


FIGURE 3: Two elemental areas in arbitrary configuration where  $i=1$  and  $j=2$ . Arrows are normal vectors to respective surface.

Two other important relationships regarding view factors are presented in equation 5. These are valid for surfaces in an enclosure.

$$\begin{cases} A_i F_{ij} = A_j F_{ji} \\ \sum_{j=1}^N F_{ij} = 1 \end{cases} \quad (5)$$

In order to calculate heat generated by radiation in an enclosure of  $N$  surfaces a total of  $N^2$  view factors are needed. However each view factor does not need to be directly calculated due to symmetries and relationships in equation 5.

Algebraic relations for some 3D geometries are tabulated and available from Howell (2010, [13]). From these tables view factors for aligned parallel rectangles and perpendicular rectangles with common edges may be calculated [11]. By using these together with the relations in equation 5 each factor can be obtained.

## 6 Finite Volume Method

The Finite Volume Method (FVM) is a tool to transform a set of partial differential equations into a system of linear algebraic equations. The discretization procedure integrates and transforms the partial differential equations into a balance equation over an element. Surface and volume integrals are transformed to discrete algebraic relations over elements and surfaces which yield a set of semi-discretized equations. Thereafter interpolation profiles are chosen to approximate the variation of the variables within an element so that surface values can be transformed to cell values [14].

## 6.1 Discretization schemes

In order to derive useful forms of the differential equation, interface properties and gradient of the temperatures at each surface is required. The six faces are labelled as east, west, north, south, top and bottom, further on referred to as E/W/N/S/T and B, see figure 4 for illustrative example in 2D.

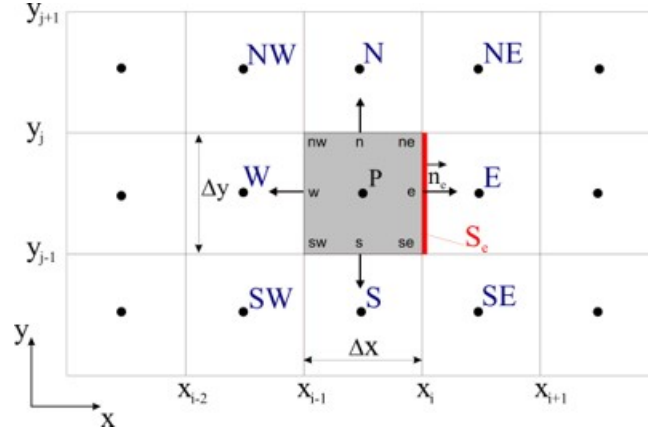


FIGURE 4: Illustration of labels for nodes [15].

Temperature values and properties are defined and evaluated at nodal points. Property variation needs to be approximated across boundaries in order to calculate fluxes at control volume faces. There are several ways of doing this. Linear approximation is a simple way of calculating interface values and gradients [14]. This type of scheme is called central differencing. It satisfies fundamental properties like conservativeness, boundedness and transportiveness, required for stability. However, the scheme does not consider the direction of the flow, which is important especially for highly conductive flows. Linearly interpolated values for the property  $\Phi$  may be evaluated as in equation 6 and the flux terms as in 7. Property values at each cell boundary is thereby calculated as an averaged value between the nodal points.

$$\Phi_w = \frac{\Phi_P + \Phi_W}{2} \quad (6)$$

$$\begin{cases} \left. \frac{\partial T}{\partial x} \right|_w \approx \frac{T_P - T_W}{\Delta x_{WP}} \\ \left. \frac{\partial T}{\partial x} \right|_e \approx \frac{T_E - T_P}{\Delta x_{PE}} \end{cases} \quad (7)$$

Subscript P stands for a general nodal point and W/E/N/S/T/B for nodal points in corresponding direction. In order to validate the accuracy of the solution a grid dependence check has to be made. If nodes are added and the solution differs from the one obtained a finer mesh has to be used for accurate results.

## 6.2 Explicit and implicit schemes

Time dependent problems require methods for integration over time. Amongst these methods are the explicit, implicit and semi-implicit schemes. The explicit scheme only uses values at the current time to predict the temperature at a later time step. It is based on backward differencing and its error accuracy is first order with respect to time. However, there are some limitations with this method. There is a maximum limit in time step  $\Delta t < \rho c_p \frac{(dx)^2}{2k}$  which is why it is not recommended for general

transient problems. If the time step is chosen with care, the explicit scheme may be efficient tool for conduction calculations [12].

The fully implicit scheme only uses values of the next time step in order to estimate the new value. This method is unconditionally stable for all time steps. The accuracy is just like the explicit scheme, first order with respect to time, which requires small time steps to ensure accuracy. Due to the implicit scheme robustness and unconditional stability it is recommended for general purpose transient calculations [12]. However, this method requires internal iterations which increases the computational cost in comparison to the explicit scheme.

## 7 Energy balance

The energy equation will be solved by using the finite volume method, explained further in this section. First law of thermodynamics state that the change in internal energy is equal to added heat minus the work done by the system. Applying this on an infinitesimally small element illustrated in figure 5 leads to relation 8.

$$\text{Rate of change of energy inside the fluid element} = \text{Net flux of heat into the element} + \text{Rate of work done on element due to body and surface forces} \quad (8)$$

The first term represent the dynamic change of energy in the element. Assuming static elements lead to equation 9 using  $\rho$  for the material density and  $c_p$  for heat capacity.

$$\text{Rate of change inside fluid element} = \rho c_p \frac{\partial T}{\partial t} dx dy dz \quad (9)$$

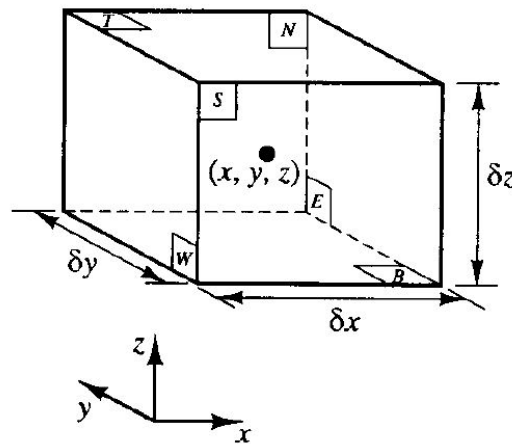


FIGURE 5: A fluid element [15].

The last term of relation 8 can be neglected, due to the static assumption of steam and solids. The second term however, will include heat fluxes due to absorption or emission of radiation and heat transfer across surfaces due to temperature gradients (like thermal conduction and convection).

As seen in figure 5 the heat transferred by thermal conduction across the x-axis will be the following.

$$(\dot{q}_x - (\dot{q}_x + \frac{\partial \dot{q}}{\partial x} dx)) dy dz = - \frac{\partial \dot{q}}{\partial x} dx dy dz \quad (10)$$

For the full 3D case, after implementing equation 2 for  $q$ , equation 11 is obtained.

$$\begin{aligned} \text{Heating of element by} \\ \text{thermal conduction} \end{aligned} = \left( \frac{\partial}{\partial x} k \frac{\partial T}{\partial x} + \frac{\partial}{\partial y} k \frac{\partial T}{\partial y} + \frac{\partial}{\partial z} k \frac{\partial T}{\partial z} \right) dx dy dz \quad (11)$$

Consequently the equation to be solved for the solids is equation 12. Note that boundary faces will have different equations.

$$\rho c_p \frac{\partial T}{\partial t} = \frac{\partial}{\partial x} k \frac{\partial T}{\partial x} + \frac{\partial}{\partial y} k \frac{\partial T}{\partial y} + \frac{\partial}{\partial z} k \frac{\partial T}{\partial z} \quad (12)$$

The partial differential equations will differ somewhat for the top layer since radiation and convection of air need to be considered, see equation 13. After some rearranging and accounted influence from the radiating source term, the equation will become:

$$\rho c_p \frac{\partial T}{\partial t} = \frac{\partial}{\partial x} k \frac{\partial T}{\partial x} + \frac{\partial}{\partial y} k \frac{\partial T}{\partial y} + \frac{\partial}{\partial z} k \frac{\partial T}{\partial z} + \frac{h_{air} \partial x \partial y}{\partial x \partial y \partial z} (T - T_{air}) + \frac{S_{radiation}}{\partial x \partial y \partial z} \quad (13)$$

The source term accounts for the energy leaving the top cells through radiation. Below is the radiation defined as the energy leaving the top surface, see equation 14.

$$S_{radiation} = \varepsilon \sigma A_{xy} T^4 \quad (14)$$

# Method

The complexity of the problem required a division into several sub calculations. The first step was to obtain the dynamic change of solid temperature. In the second step the heat balance equation was solved for steam to obtain the dynamic change of steam temperature and pressure. Consequently view factors were calculated to couple the previous balances. Boundary conditions were updated and the dynamic change of temperatures depend on each other.

## 8 Geometrical description

The geometrical description of the solids and surrounding walls are described according to dimensions of furnaces manufactured by Dongfang Boiler (DFB) [16].

The furnace is quadrangular and solids have a total weight of 150 tonnes. The bed is 9.81 meters long, 9.81 meters wide and 31.02 meters high. During electricity loss the height occupied by the solids will be 0.86 meters. Wall thickness is 1.5 centimetres and tube diameter 2 centimetres [6]. Steam walls are modelled in two dimensions. See figure 6 for the simplified geometry.

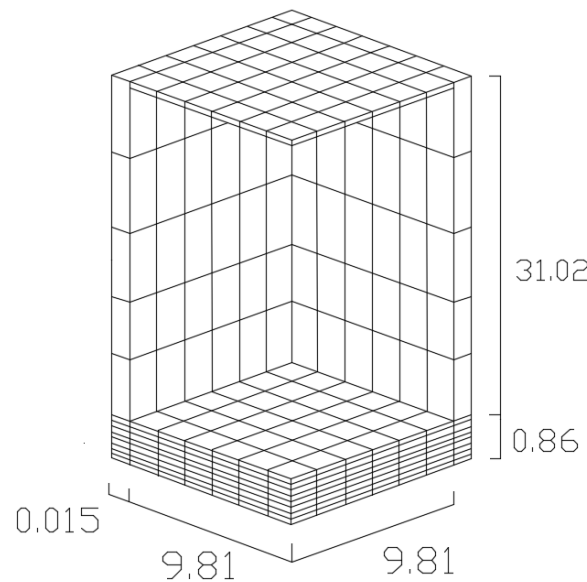


FIGURE 6: Simplified geometry and mesh of furnace [1].

## 9 Energy equation for solids

In order to solve the equations discussed in section 7, each term has to be discretized. Therefore equations 12 and 13 are integrated over the control volume and a time interval from  $t$  to  $t+\Delta t$ . Integration over the control volume means that heat fluxes need to be evaluated at the faces. The total amount of heat absorbed or emitted in a cell is determined by  $Q_{sum}$ . Calculation of  $Q_{sum}$  depends on whether the current cell P is in a corner, edge, face or interior. Surrounding cells are named after their direction and  $Q_{sum}$  is created as a sum defined in equation 15.

$$Q_{sum} = Q_e - Q_w + Q_t - Q_b + Q_n - Q_s \quad (15)$$

Each  $Q$  may have a different form depending on their direction and position. Calculated  $Q_{sum}$  will be used to update the bed temperature as following:

$$\rho_{bed} c_{p,bed} \frac{T_{bed}(x, y, z, t + \Delta t) - T_{bed}(x, y, z, t)}{\Delta t} \Delta x \Delta y \Delta z = Q_{sum} \quad (16)$$

### 9.1 Discretization schemes

The conduction term in x-direction will be evaluated as following equation 17.

$$Q_e - Q_w = k_e A_{yz} \left. \frac{\partial T}{\partial x} \right|_e - k_w A_{yz} \left. \frac{\partial T}{\partial x} \right|_w = k_e A_{yz} \frac{T_E - T_P}{\Delta x_{PE}} - k_w A_{yz} \frac{T_P - T_W}{\Delta x_{WP}} \quad (17)$$

This procedure is applied in each direction. Heat fluxes are evaluated at the faces and the method used to estimate properties was the central difference scheme. The gradient at the mid point (e) between point P and E is evaluated using this specific scheme. Accuracy is second order [14].

Assumptions must be made in order to estimate the temperature variation with time. Temperatures at time  $t$ , time  $t+\Delta t$  or a combination of these may be used to calculate the temperature at the following step. When only using the current time temperatures the scheme is called explicit, a combination is called implicit and if only temperatures at later time is used it is called fully-implicit. According to Moukalled, Mangani and Darwish [14] the explicit scheme is shown to be efficient for conduction calculations, and considering the advantage with computational cost this scheme will be the one used for further calculations [14]. Discretization of the time dependent term will be evaluated as in equation 18 and the temperatures on the right hand side of equations 12 and 13 will be evaluated at current time  $t$ .

$$\frac{\partial T}{\partial t} = \frac{T_P(x, y, z, t + \Delta t) - T_P(x, y, z, t)}{\Delta t} \quad (18)$$

### 9.2 Boundary conditions

After evaluating the discretized form of the energy equation there are inevitably some difficulties. For example either a temperature or energy flux is required at the faces, edges and corners. Since there are no temperatures defined outside the mesh, equations can not yet be solved.

A heat flux was chosen to be defined as the boundary condition and several heat transfer mechanisms have to be considered. Namely convection of steam, thermal conduction through the wall and contact resistance. Contact resistance consider

the actual surface area that is in contact. This arise due to non flatness and roughness of the contacting surfaces.

$$R_{tot} = \frac{1}{h_{steam}} + \frac{d_{wall}}{k_{wall}} + R_{contact} \quad (19)$$

Equation 19 is a measure for the total resistance used in equation 20 which allows the boundary condition to change with time together with the dynamic change of steam and bed temperatures. Note that the steam position corresponds to a position parallel to the bed cell.

$$q_{boundary} = - \frac{T_{steam}(x, y, z, t) - T_{bed}(x, y, z, t)}{R_{tot}} \quad (20)$$

Boundary conditions will depend on the type of cell; corner, edge, face or interior. For top boundary cells radiation and air convection needs to be considered therefore equation 21 is needed.

$$Q_t = \sigma \epsilon A_{xy} T_{bed}(x, y, z, t)^4 + h_{air} A_{xy} (T_{bed}(x, y, z, t) - T_{air}(t)) \quad (21)$$

Interior cells will only consider conduction in each direction as described in equation 17. For bottom corners; three parts of  $Q_{sum}$  will consist of the pre calculated heat flux  $q_{boundary}$ , as in equation 20. Top corners will have two  $q_{boundary}$  parts and one part ( $Q_t$ ) representing the radiation and convection of air, see equation 21. Top edges will consist of one boundary type of equation 21 and one of equation 20 while bottom edges will have two of the form in equation 20. Lastly, all faces except top will have one boundary condition of the form as in equation 20 while the top surface will consider radiation and air convection as in equation 21.

## 10 Energy equation for air

Air is cooled by convection to walls and heated by solid top surface according to equation 22.

$$\rho_{air} V_{air} c_{p,air} \frac{T_{air}(t + \Delta t) - T_{air}(t)}{\Delta t} = -A_{walls} \frac{T_{air}(t) - T_{means}(t)}{R_{tot,air}} + A_{bedsurface} h_{air} (T_{meanb}(t) - T_{air}(t)) \quad (22)$$

Average steam and bed temperatures are used, with subscripts means and meanb.  $R_{tot,air}$  takes the resistance of convection of air, steam and conduction of walls into account, see below.

$$R_{tot,air} = \frac{1}{h_{steam}} + \frac{d_{wall}}{k_{wall}} + \frac{1}{h_{air}} \quad (23)$$

## 11 Energy equation for steam

After obtaining temperature changes in each solid cell the steam walls can be modelled. Heat fluxes are extracted from previous solution and arranged to fit a defined number of wall segments for the conductive heat transfer. Thereafter segments in the radiating part are defined. Each surface is labelled and arranged into a three dimensional matrix. The outer part of the steam wall is assumed to be isolated.



First number of wall segments in the conductive section are defined as number of height ( $p_z$ ) and width segments ( $p_y$ ). Thereafter solids top surface is arranged to have the number of elements  $p_y$  across the width and  $p_y$  across the length. Top surface temperatures are estimated for each time step. Energy transferred through the wall to the steam side is gathered in  $q_{co}$ .

Secondly the number of wall segments in the radiating section are defined as number of height ( $p_{z2}$ ) and width segments ( $p_{y2}$ ). These numbers are used to calculate view factors from top surface to each wall segment. See Appendix 17 for a thorough explanation. View factors are used to estimate the radiating energy uptake in one wall segment from the whole solid surface. This energy uptake is labelled  $q_r$  and used to update the steam temperature together with  $q_{co}$ , see equation 24.

$$\rho_{steam} C_{p,steam} \frac{T_{steam}(x, y, z, t + \Delta t) - T_{steam}(x, y, z, t)}{\Delta t} \Delta x \Delta z d_{tube} = q_{co/r} + Q_{conduction}(x, z, t) \quad (24)$$

$$Q_{conduction}(x, z, t) = k_t(x, z, t) A_{xd_{tube}} \frac{\partial T}{\partial x} - k_b(x, z, t) A_{xd_{tube}} \frac{\partial T}{\partial x} + k_e(x, z, t) A_{xz} \frac{\partial T}{\partial z} - k_w(x, z, t) A_{xz} \frac{\partial T}{\partial z} \quad (25)$$

In equation 24 either  $q_{co}$  or  $q_r$  is used depending on if current wall is in contact with the conductive or radiating area. Besides, the term  $Q_{conduction}$  in equation 25 includes the heat transferred through conduction between cells in each direction. Heat conductivity,  $k$ , is estimated using central differencing. With current cell pressure and temperature the heat conductivity is obtained. The boundaries are considered to be isolated. No heat is transferred through the inlet, outlet or sides.

## 12 Initial conditions

It is assumed that electricity loss occurs at initial time with bed material accumulated in the bottom of the furnace having the same initial temperature. The air above is assumed to have the same initial uniform temperature. The constructed MatLab program allows the steam temperature to be defined as constant or as a temperature profile.

Initial conditions are gathered in table 1. All necessary information is given in order to solve the differential equations. Heat flux in each cell is stored as a function of time.

TABLE 1: Initial conditions.

	Initial temperature [C]	Pressure [MPa]
<b>Bed</b>	850	0.1
<b>Air</b>	850	0.1
<b>Steam</b>	in-336 out-414	in-26.5 out-25.9

Initial conditions were based on operating conditions for 350 MW CFB boilers. Inlet and outlet steam temperatures and pressures are defined [16] [6] [17]. Initial steam temperature profile was calculated by linearizing data. Note that the cells are sparser for the radiating section which has to be considered. The same procedure was performed to obtain the initial pressure profile, see figure 7.

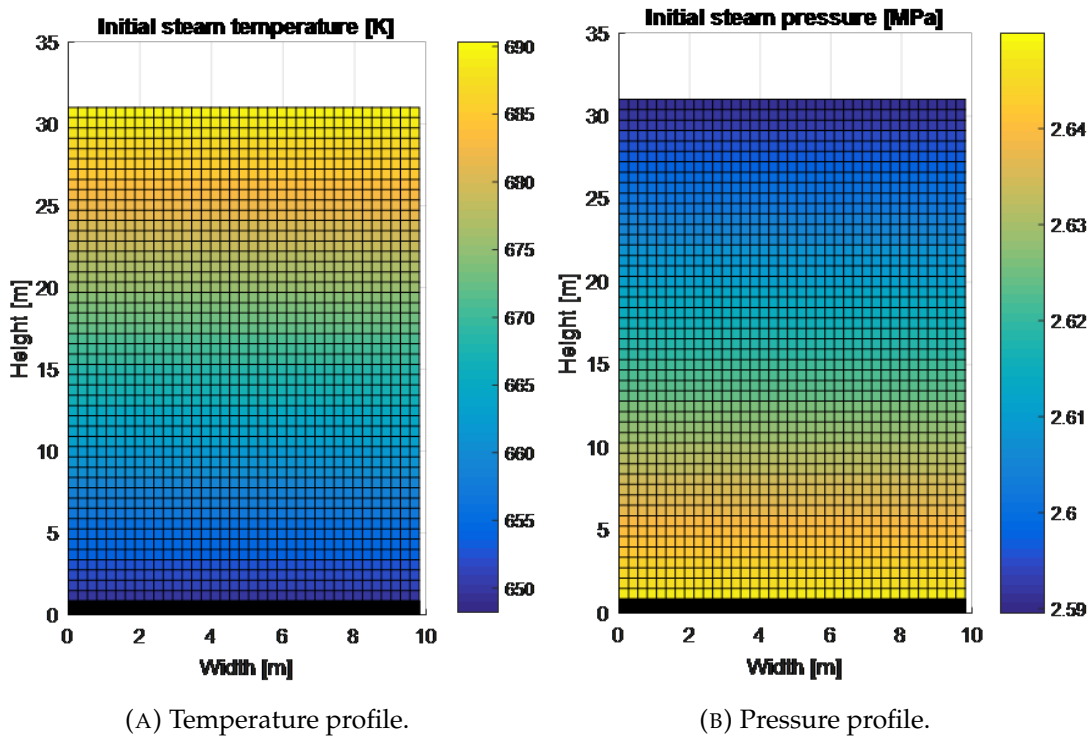


FIGURE 7: Initial profiles for one vertical wall.

The steam wall consist of 40 cells across the width. Heightwise the radiating part consists of 50 cells while the conductive part has 40 cells, which is why the bottom part of the figure is more dense.

The final simulation had constants and settings defined in tables 2 and 3. Initial time step was set to 0.05 seconds and changed after 4000 iterations to 0.10 seconds.

TABLE 2: Values of constants.

Constants	Value	Unit
$\sigma$	5.67036713e-8	W/m <sup>2</sup> K <sup>4</sup>
$\pi$	3.141592	-
$g$	9.81	m <sup>2</sup> /s
$R$	287.05	J/kgK
$R_c$	6e-4	m <sup>2</sup> K/W
$\Delta t$	0.05   0.10	s
<i>Number of cells in bed</i>	64000	-
<i>Number of cells in one wall</i>	3600	-

Heat conductivity of stainless steel is changing with temperature according to equation 26, where T is given in degrees Celsius [18].

$$k_{steel}(T) = 14.6 + 0.0127T \quad (26)$$

Equation 26 was used to estimate a mean conductivity since the values do not change drastically with time. Stainless steel has a melting point around 1673K and starts to loose strength above 673K [18]. Water walls are suitable to use for steam conditions

up to 868K-923K from a creep strength point of perspective [19]. Since ultra super critical boilers currently are developed steam walls have become more tolerant.

Air density is designed to follow the ideal gas law, see below:

$$\rho_{air}(t) = \frac{PM_{air}}{RT(t)} \quad (27)$$

Other air properties are considered to be constant in time. Heat capacity is evaluated at 800K [20] and heat transfer coefficient estimated to be 25 W/m<sup>2</sup>K [21].

Bed material consist of silica sand and air. Sand properties are constant in time and properties obtained from AZoM, online publication for the *Materials Science Community* [22]. All properties are gathered in table 3.

TABLE 3: Properties for wall, air, steam, sand and bed material.

Properties	Symbol	Sand	Air	Bed	Steam	Walls	Unit
Bed porosity	$\alpha$	0.7	-	-	-	-	%
Heat conductivity	k	1.4	0.095	1.0085	<i>CoolProp</i>	21.9025	W/mK
Heat capacity	$c_p$	800	1100	890	<i>CoolProp</i>	-	J/kgK
Heat transfer coeff.	h	-	25	-	100	-	W/m <sup>2</sup> K
Molar mass	M	-	0.029	-	-	-	kg/mol
Density	$\rho$	2650	$\rho_{air}(T)$	1855	<i>CoolProp</i>	-	kg/m <sup>3</sup>
Emissivity	$\varepsilon$	-	-	0.8	-	0.8	-

The dynamic steam properties are evaluated with CoolProp which is a C++ library storing properties of pure and pseudo-pure fluids. These fluids cover a wide range of industrial heat transfer media. Hence a majority of the fluids cover extreme temperatures. *CoolProp* license cover academic works [23] and is applicable in MatLab.

### 13 Code structure

The final code was developed to be as general as possible. It consists of one main script, several functions and one database. The main script allows properties for bed material, air and walls to be defined. Either constant or dynamic with temperature. Steam properties are estimated with the database *CoolProp* and initial conditions can be defined as either constant or linearized. Initial time step can be set in the beginning but allowed to be altered during simulations. The geometry of the furnace may have any quadrangular form. Number of cells in each direction for the solids is defined first. Thereafter number of cells for steam walls are required to be the same across the width but altered at height. Different values can be chosen for conductive- and radiating part.

After these conditions are set one function will calculate view factors, which will be used for calculation of radiating heat flux. The code will enter the time loop and firstly update each solid cell temperature which is followed by air temperature update. Thereafter conductive heat flux will be extracted and radiating heat fluxes calculated. Finally steam temperature will be updated, thereafter the boundary conditions and this procedure will be repeated until finished.

There are possibilities for this code to be widely applied. For example, different type of solids could be investigated and their heat transfer compared. If more time were to be available different initial conditions and more complex heat transfer mechanisms would be considered.

## Results and discussion

This section will present the results and discuss the dynamic change of air, bed and steam. Figure 8 shows the air temperature. It is quickly cooled by the surrounding walls and after approximately 30 seconds it is heated from the solid surface until it reaches a steady temperature of 705 K (432°C). The cooling of the top surface is a slower process compared to the steam temperature increase, which is why the air is heated after a while.

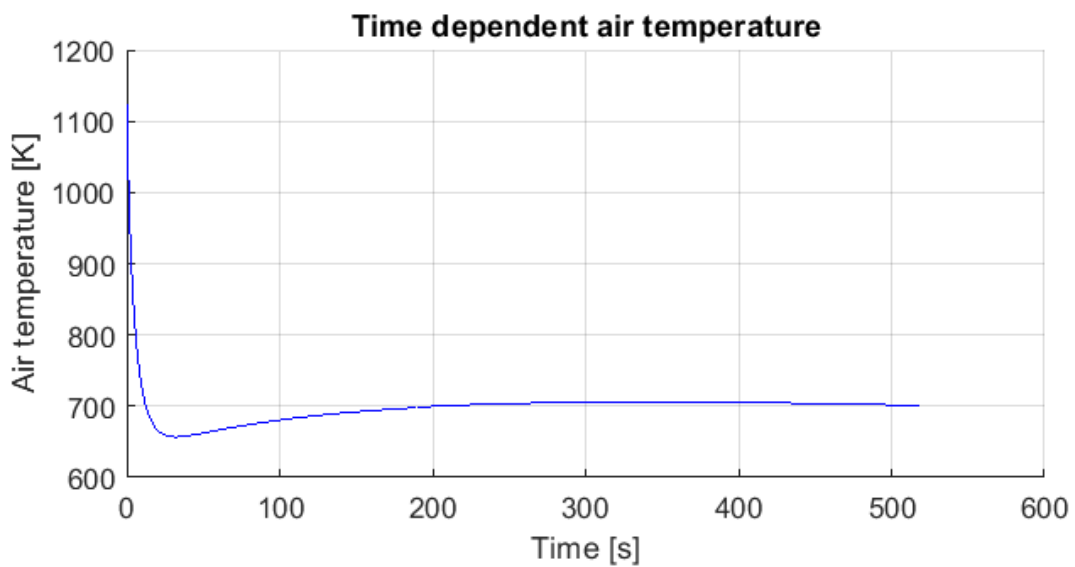


FIGURE 8: Temperature profile for air.

If air were to have flue gas properties other results may be expected. In that case emissivity should be considered, which would result in additional radiation to the surrounding walls. Some radiation emitted from the solids would also be absorbed. Additionally, flue gas properties are somewhat difficult to estimate since they depend on fuel composition and temperature. In CFB boilers air is supplied which keeps the solids in a suspension, this air is mixed with flue gases during normal operation. Air and flue gas amount and composition will change during electricity loss which makes the process complex. Therefore it is difficult to evaluate what the profile would look like in case of flue gas. In order to further increase accuracy it would be convenient to split the air into several cells.

## 14 Dynamic solid progress

Dynamic change of temperature in different bed cells are introduced in figure 6. Bed cells are labelled according to x-, y- and z-coordinates in metric units and different positions are investigated.

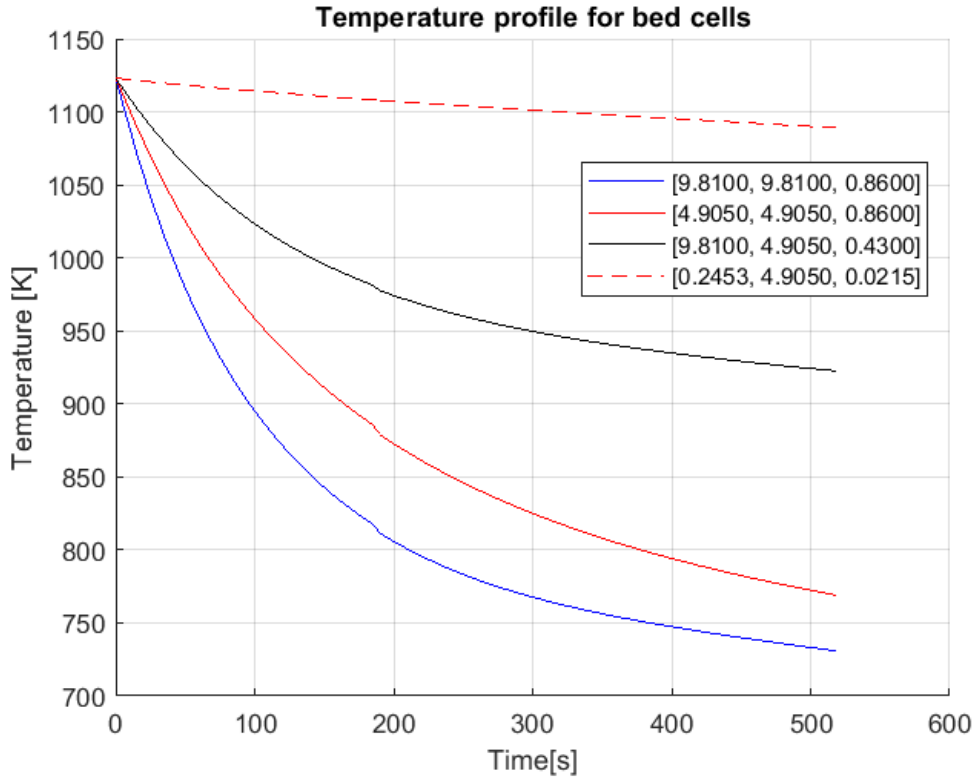


FIGURE 9: Temperature profile for solids.

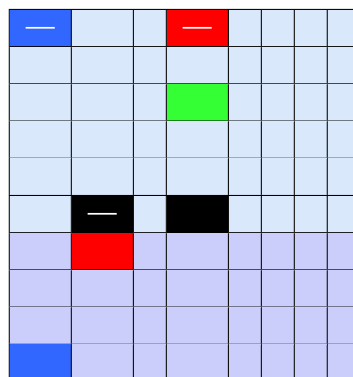
It is clear that top corner cell, labelled [9.81, 9.81, 0.86], is cooled faster in comparison to other parts. Probably due to the fact that it is cooled by conduction to the walls on two sides and radiation on top. It is followed by top middle cell [4.905, 4.905, 0.86] and lastly face middle cell [9.81, 4.905, 0.43]. Top surface is initially cooled faster considering the large temperature differences which drives the heat transfer. Since radiation has a  $T^4$  dependence it is more sensitive to temperature changes. Thus it is cooled exponentially in comparison to conductive cells which have a linear temperature dependence. The slope of the bed cell temperature decreases after approximately 400 seconds and temperatures become more even. Nonetheless, equilibrium has not been reached. It is interesting to notice that the bed surface temperature is approaching a steady temperature around the same stabilised air temperature.

Figure 9 shows that the bottom corner is cooled much slower and therefore a large amount of time will be needed before reaching equilibrium. The critical point for the steam in the conductive area would therefore be in the bottom corner.

One assumption regarding the solids was that it consists of silica sand. However a more realistic scenario would be to include properties of fuel. It is possible that some combustion will occur inside the static solids even after electricity loss due to the high temperatures and presence of residue oxygen. This would result in a source term continuing to heat each solid cell. Energy created from combustion

## 15 Dynamic steam progress

TABLE 4: Placement of temperature 1D profiles.



The dynamic progress of different cells defined by width and height coordinates are presented in figure 10.

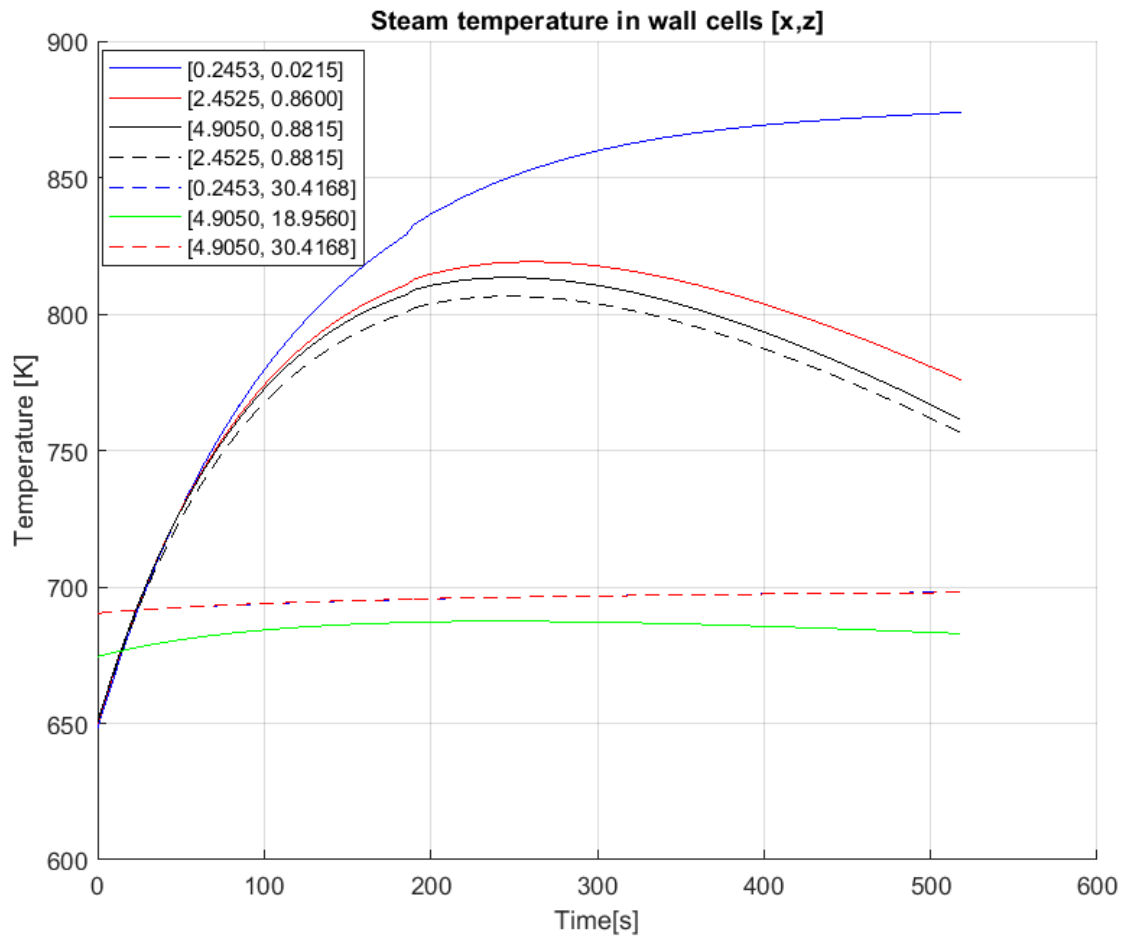


FIGURE 10: Temperature profile in south steam wall.

It can be observed in figure 10 that upper part of the walls are less sensitive to radiation (red and blue dashed lines and green solid line). Parts closer to the solid surface are more exposed and vulnerable to radiation. Highest temperatures are reached in these areas after approximately 240 seconds. Maximum temperature achieved is 820 K. At this time figure 9 shows that the slope of the top cell temperature [ $x=9.81$ ,  $y=9.81$ ,  $z=0.86$ ] and middle surface temperature [ $x=4.905$ ,  $y=4.905$ ,  $z=0.43$ ] decrease.

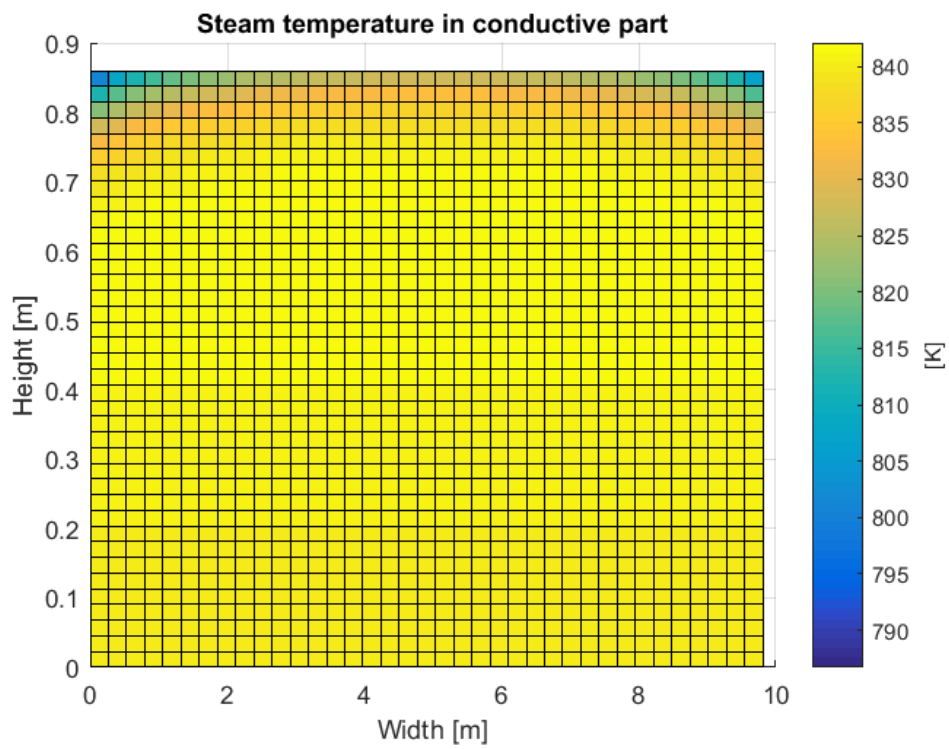


FIGURE 11: Conductive area after 200 seconds.

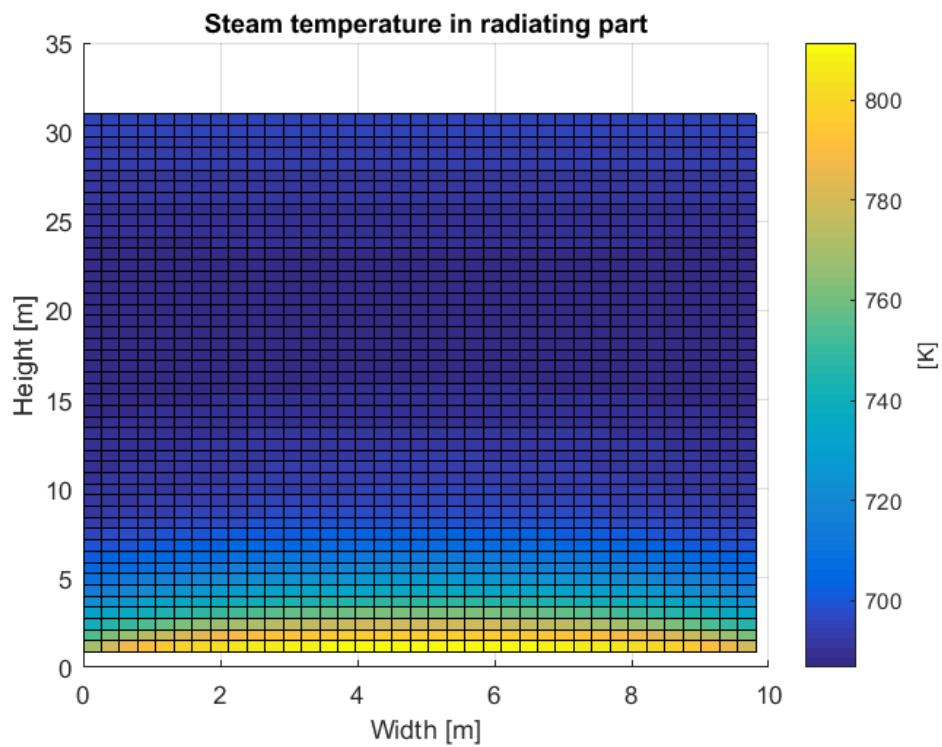


FIGURE 12: Radiating area after 200 seconds.

Surface plots of steam temperatures in south wall are presented in figures 11 and



12. The trends of the temperature are clear. The conductive part has shown to have higher temperatures, as seen in the different limits of the colour bar between the figures. The maximum temperature in the conductive part goes up to 875K and is still increasing. Since top corner solid cells are cooled faster it will result in lower steam temperatures in the upper corner of the conductive area. The highest temperatures achieved in the radiating part is located in the bottom center cells.

Walls are suitable for steam temperatures up to 868K - 923K. Therefore it is difficult to estimate precisely which temperature would cause the tubes to burst. However, results show that the maximum temperature achieved is located in the middle of the acceptable span. According to these simulations it would take around 280 seconds until this maximum temperature is reached. Since there is no data from real cases it is difficult to compare these results with reality.

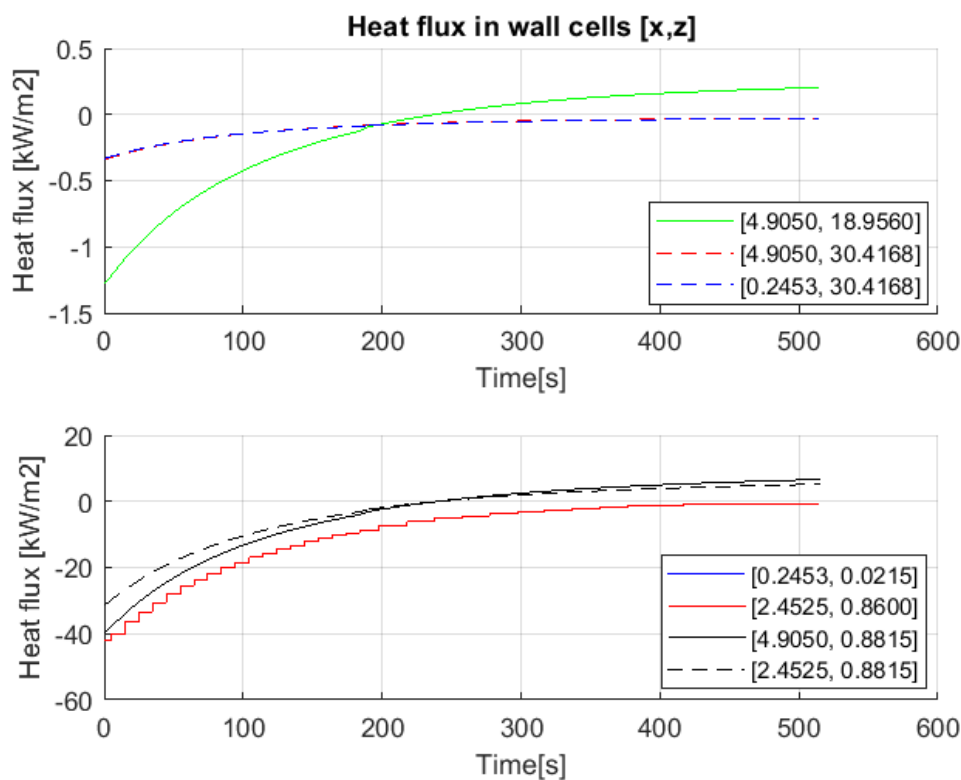


FIGURE 13: Heat transferred through south steam wall.

Figure 13 shows how much energy has been transferred in each cell. In order to compare these results the total amount of heat has been divided by respective area.

Top wall cells receive less energy compared to the conductive heat. It is also observed that the heat transfer will change direction in some parts and steam will begin to heat the furnace after approximately 200 seconds. This is observed in the top sub figure where the green line heat transfer reaches zero after 200 seconds. This also explains why the slope of the bed cell temperatures start to decline.

The bottom sub figure shows that the heat received in the conductive part is the largest. The most critical area will therefore be in the bottom corners, since the bed temperature in these areas will be the largest for the longest time. The highest temperatures achieved in the conductive part lies around 875 K and is still increasing.

## 16 Simulation process

MatLab was shown to be very slow with increasing number of cells which is why the code had to be separated and restarted with new initial conditions every 200 iteration. In the end each file had to be loaded and relevant results gathered. Another way to overcome this would be by restructuring or simplifying the code or perhaps use the program *Fortran*. This was one of the reasons why momentum and mass balances were neglected. After running and timing each section it was shown that the function which updates the steam temperature in the radiating part takes the longest time. This part was restructured and simplified but still took up the largest amount of time.

Time step of 0.05 seconds was used for 4000 iterations. The time step 0.10 seconds was tested for 100 iterations and by comparison the difference was acceptably low, indicating that it is valid for usage. Therefore iterations were continued with time step 0.10 seconds.

Different mesh sizes were investigated. Fewer cells were shown to give different results. By increasing number of cells the number of view factors increases significantly leading to a much more time consuming code. Consequently the solution is not completely mesh independent. Due to time limitations and resources there was no room for investigating larger number of cells. By using 50 cells in radiating part the final size of view factor matrix was 11200 x 11200. However, results still indicate that there is a possibility to neglect the urgent feed water system. Due to the fact that the steam reaches temperatures between the hazard limits for the wall further studies has to be conducted.

## 17 Future work

Since feed water pump is out of power the movement of steam will be caused by pressure gradients. Therefore, a more realistic scenario would be a rising steam. This implementation would most likely result in a more even spread of energy which is taken up by the radiation. The upper part of the furnace would probably have a larger temperature increase.

One important aspect would be to include momentum equations. By solving the momentum equations steam would move upwards and the steep temperature increase between the conductive and radiating parts would most likely spread out making the result more accurate. The overall steam temperatures would be slightly decreased due to steam movement.

As previously mentioned further investigation should introduce mass- and momentum balances. Following equations should therefore be included. Mass conservation in equation 28.

$$\frac{\partial \rho}{\partial t} + \nabla(\rho \mathbf{u}) = 0 \quad (28)$$

Momentum balance in equation 29 includes forces due to pressure gradients, shear stress and gravity where  $\mathbf{u}$  is the three dimensional velocity field.

$$\frac{\partial \rho \mathbf{u}}{\partial t} + \nabla(\rho \mathbf{u} \mathbf{u}) = \rho \mathbf{g} - \nabla P + \mu \nabla^2 \mathbf{u} \quad (29)$$

Since the steam temperature increase was high but not extreme, other more economical emergency equipment might be considered. One method currently installed in

Chinese CFB boilers is the PCV, Pressure Control Valve. It is often installed at superheater outlet to prevent steam pressure from exceeding a specific value. It opens before the safety valve to avoid frequent use of the safety valve which could shorten its lifespan. During electricity loss the PCV automatically opens to reduce the steam in the walls. There are good possibilities that this implementation would be enough to ensure safety of steam walls during electricity loss. However, this field requires additional investigation.

# Conclusions

A three dimensional model of the heat transfer in CFB boilers has been developed and implemented. The model includes energy balances for air, bed materials and steam. Due to the general structure of the code there are possibilities for it to be widely applied.

The main parameter that has been investigated in this study is the temperature. Simulations shows that air stabilizes relatively fast around 705K. Bed temperatures decrease relatively fast for the upper layers while the lower parts decrease at a slower pace.

The highest temperatures achieved is located in the bottom of the furnace, the conductive part, and lies around 875 K which is still increasing. This temperature lies in the acceptable span for wall conditions. This indicates a possibility for economic savings. However, further studies are required for a conclusion about the urgent water feeding system.

# Bibliography

- [1] K. Ljungberg, *Simplified geometry, dimensions and mesh of a 350 MW circulating fluidized bed boiler*. 2018.
- [2] B. S. R. of World Energy June 2016, 2016. [Online]. Available: <https://www.bp.com/content/dam/bp/pdf/energy-economics/statistical-review-2016/bp-statistical-review-of-world-energy-2016-full-report.pdf>.
- [3] J. Lyu, H. Yang, and G. Yue, *Research development and its application of circulating fluidized bed boiler technology in China*, 2017.
- [4] X. J.Z. S. Gu Haiming Shen Laihong and S. Tao, "Chemical looping combustion of biomass/coal with natural iron ore as oxygen carrier in a continuous reactor", *Energy Fuels*, vol. 25, no. 52, pp. 446–455, 2011. [Online]. Available: <http://pubs.acs.org/doi/pdf/10.1021/ef101318b>.
- [5] T. Mattison, M. Keller, C. Linderholm, P. Moldenhauer, M. Ryden, H. Leion, and A. Lyngfelt, *Chemical-looping technologies using circulating fluidized bed systems: Status of development*, 2008. [Online]. Available: [http://publications.lib.chalmers.se/records/fulltext/250058/local\\_250058.pdf](http://publications.lib.chalmers.se/records/fulltext/250058/local_250058.pdf).
- [6] X.Q.G. X. Qiang, "Study on the safety of water-wall after the bt of water supply interruption of supercritical cfb boiler", *Dongfang Electric Review*, pp. 43–46, 2016.
- [7] J. Yerushalmi, "Circulating fluidized bed boilers", *Fuel Processing Technology*, vol. 5, pp. 25–63, 1981. DOI: 0378-3820/81/0000-0000. [Online]. Available: <https://goo.gl/4QJqD1>.
- [8] *What is the difference between a PC boiler and a CFB boiler?*, 2017. [Online]. Available: <https://thermodyneboilersblog.wordpress.com/2017/02/21/what-is-the-difference-between-a-pc-boiler-and-a-cfb-boiler/>.
- [9] J. Duffield, R. Nijsing, and N. Brinkhof, "Emergency pressure relief calculations using the computer package: Relief", *Journal of Hazardous Materials*, vol. 46, no. 2-3, pp. 131–143, 1996. DOI: 10.1016/0304-3894(95)00065-8.
- [10] B. Deng, *Flow chart of an emergency water supply system*. 2018.
- [11] T. L. Bergman, A. S. Lavine, F. P. Incropera, and D. P. Dewitt, *Fundamentals of Heat and Mass Transfer*, 7th ed. John Wiley and Sons, 2011.
- [12] H. K Versteeg and W Malalasekera, *An introduction to Computational Fluid Dynamics The Finite Volume Method*. Longman Scientific & Technical, 1995.
- [13] J. R. Howell, *A catalog of radiation heat transfer configuration factors*, 2010. [Online]. Available: <http://www.thermalradiation.net/tablecon.html>.
- [14] F. Moukalled, L. Mangani, and M. Darwish, *The Finite Volume Method in Computational Fluid Dynamics*. Springer International Publishing AG, 2016.
- [15] M. de Mier Torrecilla, *Introduction to numerical simulation of fluid flows*, 2016. [Online]. Available: <http://slideplayer.com/slide/4793674/>.

- [16] W. Dong—Fu and X. Kun, “Theoretical analysis and calculation of the unsteady heat transfer process of supercritical circulating fluidized bed boiler furnace under the emergency conditions”, *Boiler Technology*, vol. 46, no. 5, pp. 35–38, 2015. DOI: [10.3969/j.issn.1672-4763.2015.05.008](https://doi.org/10.3969/j.issn.1672-4763.2015.05.008).
- [17] M. Zhang, *Design and operation of 350MW CFB boiler in China*, 2016.
- [18] C. Bailey, *Structural material behavior in fire: Steel: Stainless steel thermal properties*. [Online]. Available: <http://www.mace.manchester.ac.uk/project/research/structures/strucfire/materialInFire/Steel/StainlessSteel/thermalProperties.htm>.
- [19] R. Viswanathan, R. Purgert, and U. Rao, *Materials technology for advanced coal power plants*, 2018. [Online]. Available: [https://www.researchgate.net/publication/237625573\\_MATERIALS\\_TECHNOLOGY\\_FOR\\_ADVANCED\\_COAL\\_POWER\\_PLANTS](https://www.researchgate.net/publication/237625573_MATERIALS_TECHNOLOGY_FOR_ADVANCED_COAL_POWER_PLANTS).
- [20] I. Urieli, *Specific heat capacities of air - (updated 7/26/08)*, 2008. [Online]. Available: [https://www.ohio.edu/mechanical/thermo/property\\_tables/air/air\\_Cp\\_Cv.html](https://www.ohio.edu/mechanical/thermo/property_tables/air/air_Cp_Cv.html).
- [21] *Engineering toolbox, air - thermal conductivity*, 2009. [Online]. Available: [https://www.engineeringtoolbox.com/air-properties-viscosity-conductivity-heat-capacity-d\\_1509.html](https://www.engineeringtoolbox.com/air-properties-viscosity-conductivity-heat-capacity-d_1509.html).
- [22] M. Lines, *Properties: Silica - silicon dioxide (sio2)*, 2001. [Online]. Available: <https://www.azom.com/properties.aspx?ArticleID=1114>.
- [23] I. H. Bell, J. Wronski, S. Quoilin, and V. Lemort, “Pure and pseudo-pure fluid thermophysical property evaluation and the open-source thermophysical property library coolprop”, *Industrial & Engineering Chemistry Research*, vol. 53, no. 6, pp. 2498–2508, 2014. DOI: [10.1021/ie4033999](https://doi.org/10.1021/ie4033999). [Online]. Available: <http://pubs.acs.org/doi/abs/10.1021/ie4033999>.
- [24] J. R. Ehlert and T. Smith, “View factors for perpendicular and parallel, rectangular plates”, *Journal of Thermophysics and Heat Transfer*, vol. 7, no. 1, pp. 173–174, 1993.

# Appendix A

## Calculation of $Q_{sum}$ for solids

The calculation of  $Q_{sum}$  depends on whether the current cell is in a corner, edge, face or interior cells. The surrounding cells are named after their direction.  $Q_{sum}$  is formed as a sum of these as in equation 15.

$$Q_{sum} = Q_e - Q_w + Q_t - Q_b + Q_n - Q_s \quad (30)$$

Each  $Q$  has a different form depending on their direction. Interior cells will only consider conduction in each direction. The form for  $Q_e$  will for example be:

$$Q_e = k_{bed} A_{yz} \frac{T(x + \Delta x, y, z, t) - T(x, y, z, t)}{\Delta x} \quad (31)$$

For bottom corners three parts of  $Q_{sum}$  will consist of a pre calculated heat flux called  $q_{boundary}$  see equation 32.

$$q_{boundary} = \frac{T_{steam}(x, y, z, t) - T_{bed}(x, y, z, t)}{R_{tot}} \quad (32)$$

In equation 32  $R_{tot}$  considers the resistance of steam convection, conduction and contact resistance between the wall and solids. Since this heat flux depends on bed temperature it will be updated after each time step.

Top corners will have two  $q_{boundary}$  parts and one part ( $Q_t$ ) representing the radiation and convection of air, see equation 33.

$$Q_t = \sigma \epsilon A_{xy} T(x, y, z, t)^4 + h_{air} A_{xy} (T(x, y, z, t) - T_{air}(t)) \quad (33)$$

Top edges will have one boundary of equation 33 and one of 32 while bottom edges will have two of the form in equation 32.

Lastly, all faces except top will have one boundary condition of the form as in equation 32 while the top surface will consider radiation and air convection as in 33.

# Appendix B

## View factors

Several equations were used for the calculation of view factors. A general function was made returning view factors from surface  $i$  to surface  $j$   $F(i,j)$  depending on given geometry. The available equations were used for rectangles with common edge, parallel rectangular surfaces across each other, rectangle to rectangle in a perpendicular plane and lastly rectangle to rectangle in a parallel plane. The equations for rectangles with common edge and parallel rectangular surfaces were obtained from literature [11], see equations 34 and 36 respectively.

## Rectangles with common edge

For the first defined view factor the length of the segments,  $X$ , will be the same while the width of surface  $i$  is defined as  $Y$  and the height of surface  $j$  as  $Z$ . View factor from  $i$  to  $j$  is defined below with the relevant variables defined in following equations.

$$F(i,j) = C_1[C_2 - C_3 + 0.25 \ln(C_4 C_5 C_6)] \quad (34)$$

$$H = \frac{Z}{X} \quad W = \frac{Y}{X} \quad (35a)$$

$$C_1 = \frac{1}{\pi W} \quad (35b)$$

$$C_2 = W \arctan\left(\frac{1}{W}\right) + H \arctan\left(\frac{1}{H}\right) \quad (35c)$$

$$C_3 = \sqrt{H^2 + W^2} \arctan\left(\frac{1}{\sqrt{H^2 + W^2}}\right) \quad (35d)$$

$$C_4 = \frac{(1 + W^2)(1 + H^2)}{1 + H^2 + W^2} \quad (35e)$$

$$C_5 = \left( \frac{W^2(1 + W^2 + H^2)}{(1 + W^2)(W^2 + H^2)} \right)^{W^2} \quad (35f)$$

$$C_6 = \left( \frac{H^2(1 + W^2 + H^2)}{(1 + H^2)(W^2 + H^2)} \right)^{H^2} \quad (35g)$$

## Parallel surfaces across each other

The view factor for parallel surfaces is similarly defined. The length ( $X$ ) and width ( $Y$ ) of the surfaces are the same and the distance between the plates is defined as  $Z$ .



View factor from i to j is computed using relevant variables in equation 36.

$$F(i, j) = C_1(C_2 + C_3 + C_4 - C_5) \quad (36)$$

$$\mathbf{X} = \frac{X}{Z} \quad \mathbf{Y} = \frac{Y}{Z} \quad (37a)$$

$$C_1 = \frac{2}{\pi \mathbf{X} \mathbf{Y}} \quad (37b)$$

$$C_2 = \ln \left( \sqrt{\frac{(1 + \mathbf{X}^2)(1 + \mathbf{Y}^2)}{1 + \mathbf{X}^2 + \mathbf{Y}^2}} \right) \quad (37c)$$

$$C_3 = \mathbf{X} \sqrt{1 + \mathbf{Y}^2} \arctan \left( \frac{\mathbf{X}}{\sqrt{1 + \mathbf{Y}^2}} \right) \quad (37d)$$

$$C_4 = \mathbf{Y} \sqrt{1 + \mathbf{X}^2} \arctan \left( \frac{\mathbf{Y}}{\sqrt{1 + \mathbf{X}^2}} \right) \quad (37e)$$

$$C_5 = \mathbf{X} \arctan(\mathbf{X}) + \mathbf{Y} \arctan(\mathbf{Y}) \quad (37f)$$

## Rectangles in perpendicular plane

For view factors for perpendicular plane rectangles the formula is a bit more complicated. The dimensions of each surface ( $\xi$ ,  $\eta$ ,  $y$  and  $x$ ) are presented in figure 14. Equations are listed below [24]. Note that the equation is not valid if the surfaces share a common edge.

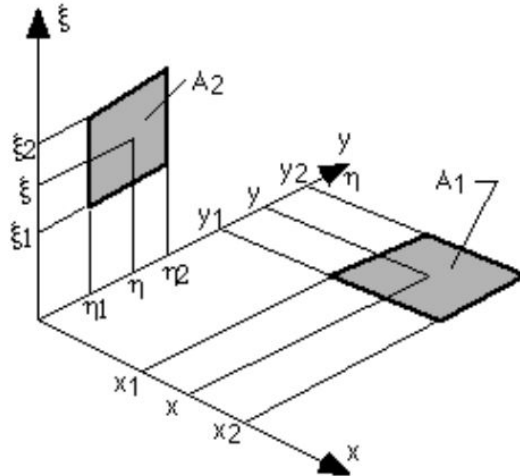


FIGURE 14: Dimensions of two perpendicular rectangular surfaces [13].

$$F(i, j) = C_1 \sum_l^2 \sum_k^2 \sum_i^2 \sum_j^2 [(-1)^{i+j+k+l} G(x_i, y_j, \eta_k, \xi_l)] \quad (38)$$

$$C_1 = \frac{1}{(x_2 - x_1)(y_2 - y_1)} \quad (39a)$$

$$K = \frac{y - \eta}{\sqrt{(x^2 + \xi^2)}} \quad (39b)$$

$$G(x, y, \eta, \xi) = \frac{1}{2\pi} \left( (y - \eta) \sqrt{x^2 + \xi^2} \arctan(K) - \frac{1}{4} (x^2 + \xi^2) (1 - K^2) \ln[(x^2 + \xi^2)(1 + K^2)] \right) \quad (39c)$$

## Parallel rectangle surfaces

The final view factor calculation is done for parallel rectangle surfaces [24]. The geometry and variables ( $x$ ,  $y$ ,  $z$ ,  $\eta$ ,  $\xi$  and  $\gamma$ ) are described in figure 15.

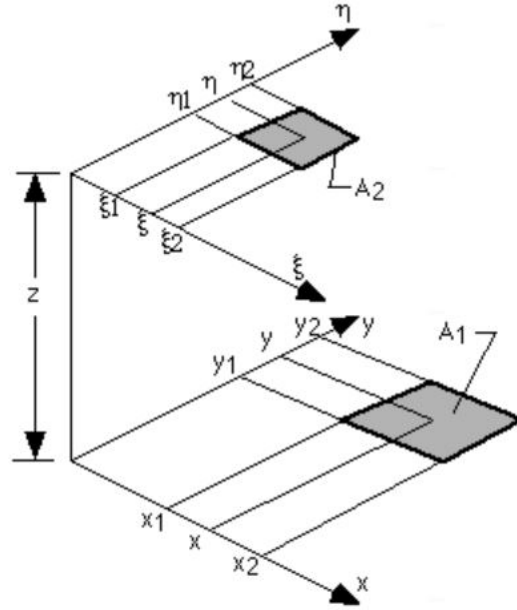


FIGURE 15: Dimensions of two parallel rectangular surfaces [13].

Calculation of  $F(i,j)$  is the same as in equation 36, however function  $G$  will differ, see below.

$$G(x, y, \eta, \xi) = \frac{1}{2\pi} \left( (y - \eta) \sqrt{(x - \xi)^2 + z^2} \arctan \left( \frac{y - \eta}{\sqrt{(x - \xi)^2 + z^2}} \right) + \right. \quad (40a)$$

$$\left. (x - \xi) \sqrt{(y - \eta)^2 + z^2} \arctan \left( \frac{x - \xi}{\sqrt{(y - \eta)^2 + z^2}} \right) - \frac{z^2}{2} \ln \left[ (x - \xi)^2 + (y - \eta)^2 + z^2 \right] \right)$$

These functions will be used to evaluate the view factors from top surface of solids to each wall segment. The calculation is divided into several parts. The dimension of each wall segment is stored in  $X$ ,  $Y$  and  $Z$ -vectors. Thereafter each segment is labelled beginning with the top surface followed by south, east, north, west walls and lastly the roof. The segments are labelled from origo, positive in  $x$ -,  $y$ - and  $z$ -directions. View factors to each roof segment is calculated using equation 36 and 40a looping over every possible combination. Thereafter the first wall segment to each perpendicular top surface segment with a common edge was calculated with

equation 34. Using symmetry factors for the whole first horizontal wall segments could be defined.

Consecutive section calculated factors for each vertical wall segment to perpendicular top segment by using equation 34 and relationships described in equation 5.

# Appendix C

## MatLab program

The final program consists of several functions, one main script and a database. Figures 16, 17 and 18 illustrate the relations between the main script and functions.

Firstly physical constants regarding geometry and properties and mathematical constants were defined. The function *meshing* was used to create a mesh for the 3D solids. Steam properties were defined to change with temperature and pressure. Thereafter initial conditions were created for the solids. Steam initial properties were created by linearizing experimental data by the function *steaminitial*. Next *qBC* was used to create boundary conditions based on solid and steam temperatures.

Before entering the time loop *generalviewfactor* calculated view factors for each surface segment, see figure 16.

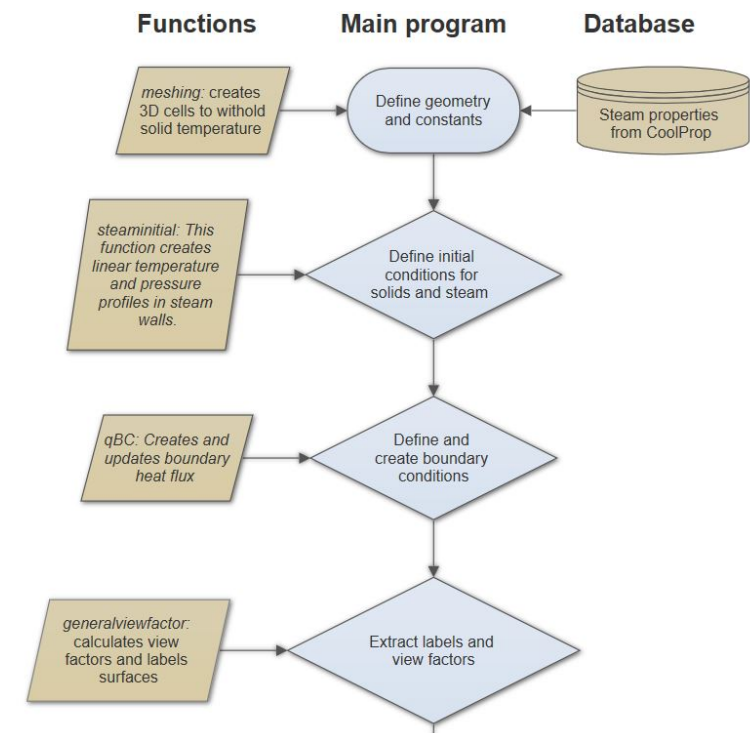


FIGURE 16: Description of MatLab functions, main file and database, part 1.

Figure 17 shows the time loop. After obtaining boundary and initial conditions differential equations could be solved. First the solid temperature in each cell was updated with *bulk*, then the air temperature with *airtemp*. *Steamtime* extracted heat fluxes to the steam and *heatrad* arranged top surface temperature.

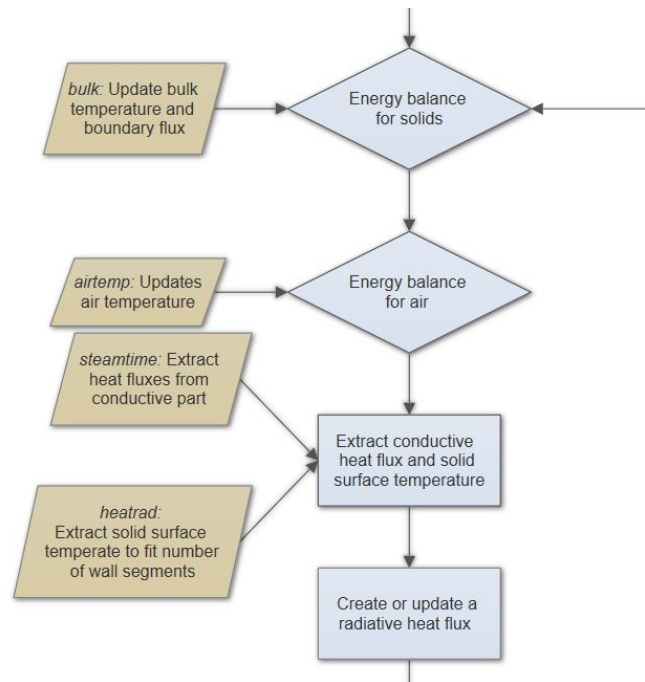


FIGURE 17: Description of MatLab functions, main file and database, part 2.

Next a matrix with radiating heat fluxes was created and lastly *steamFVM* solved for new steam temperatures, see figure 18. If time has not reached ending time then the procedure will be repeated and solved for another time step. Ultimately the results were plotted.

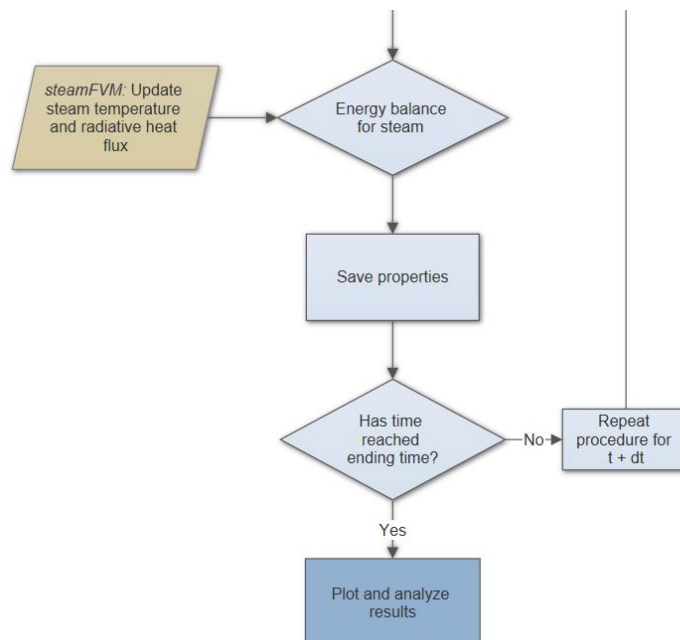


FIGURE 18: Description of MatLab functions, main file and database, part 3.

Constants and properties were saved under different class names. These included

---

steam, air, bed, sand, cons and meshcube. Other functions included but not mentioned are amongst others *see* which plots the three dimensional temperature progress in solid cells and *saveres* which loads each file and gathers results in one matrix.

# Appendix D

## Three dimensional results

3D results are presented in figures below. Figures show surface plots at different times.

## Three dimensional results for steam temperatures in conductive area

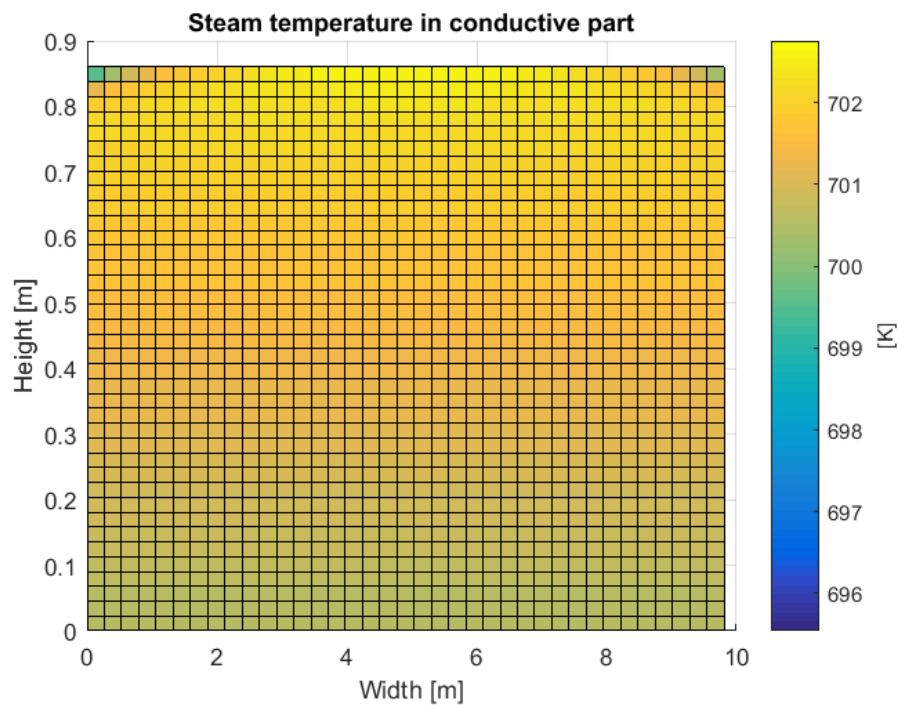


FIGURE 19: Temperature profile after 30 seconds.

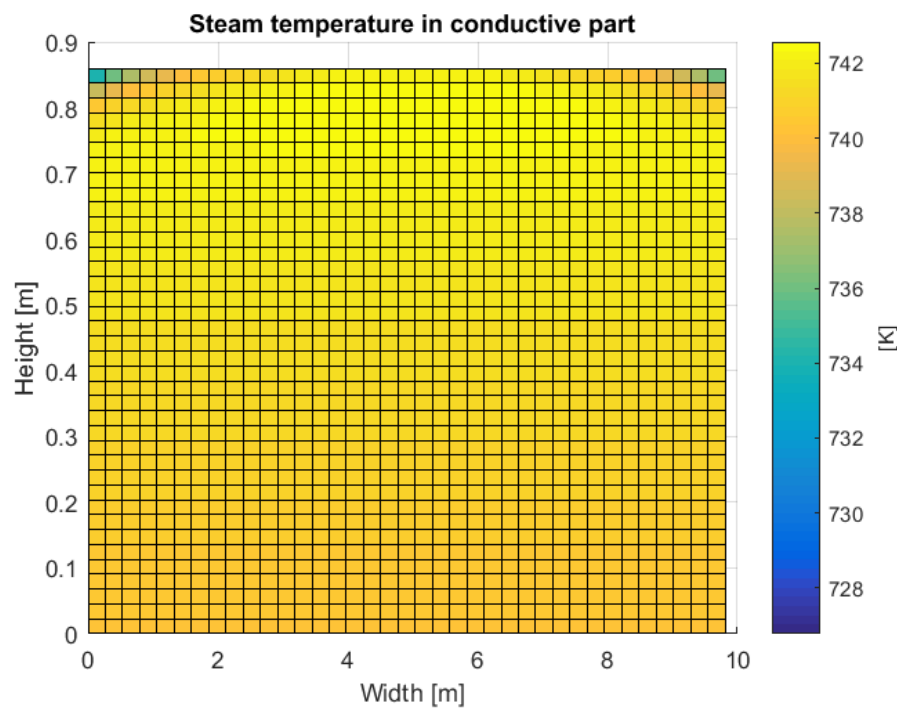


FIGURE 20: Temperature profile after 60 seconds.

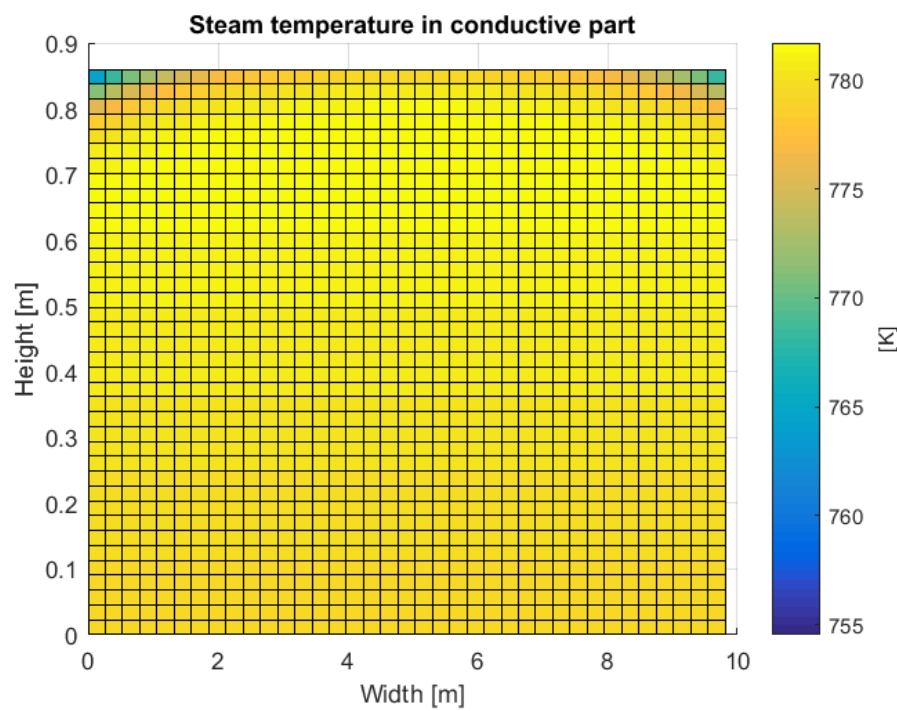


FIGURE 21: Temperature profile after 100 seconds.



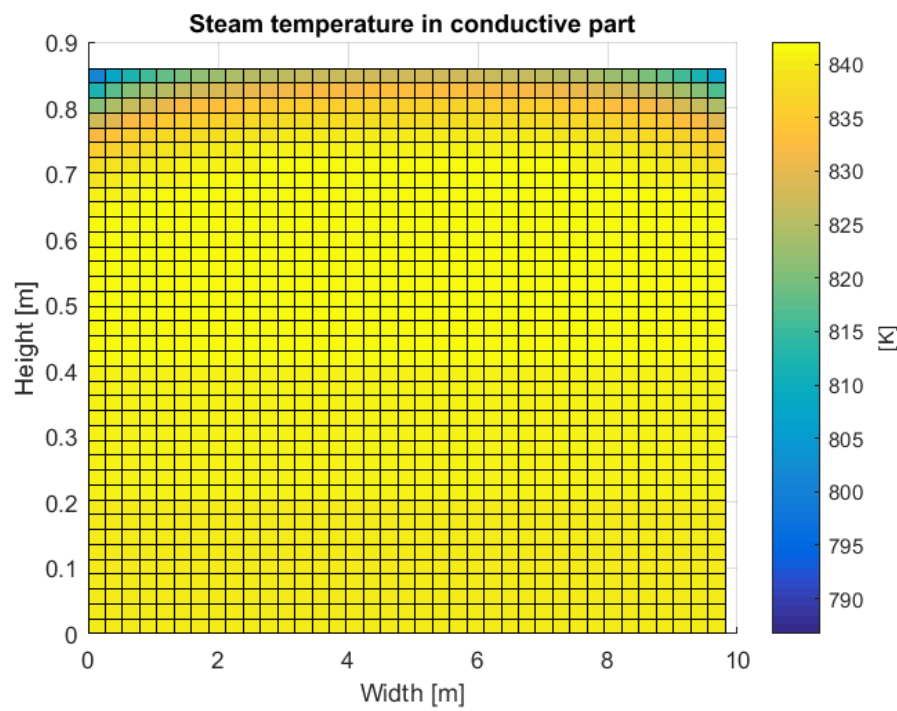


FIGURE 22: Temperature profile after 200 seconds.

Three dimensional results for steam temperature in radiating area

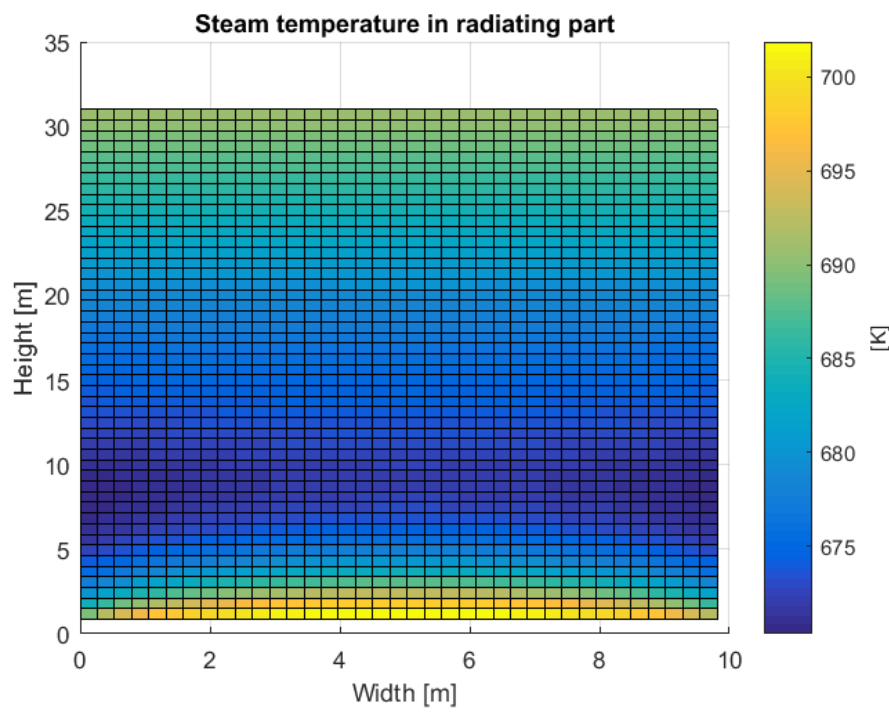


FIGURE 23: Temperature profile after 30 seconds.

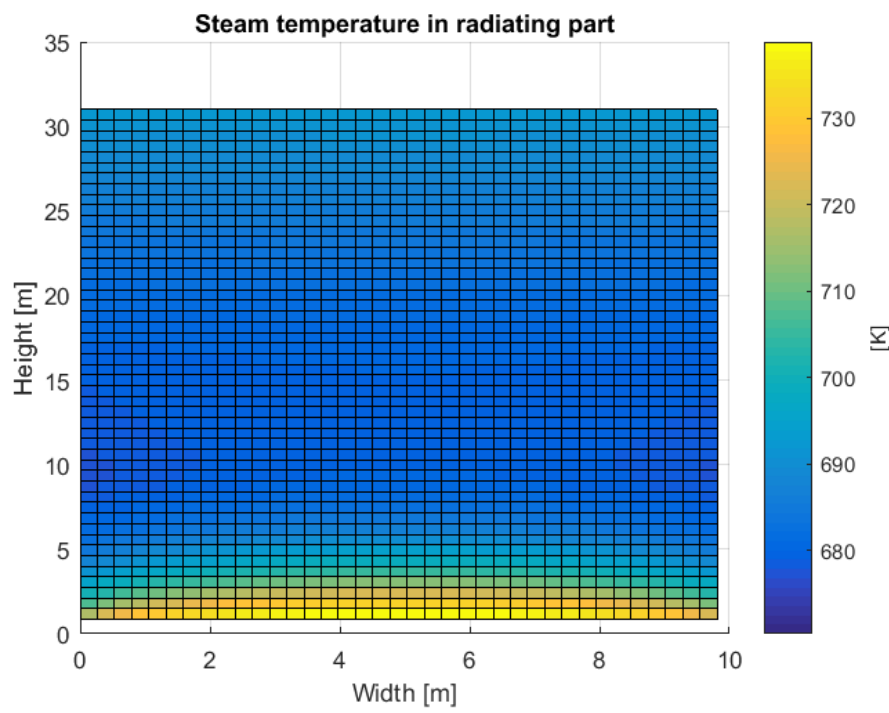


FIGURE 24: Temperature profile after 60 seconds.

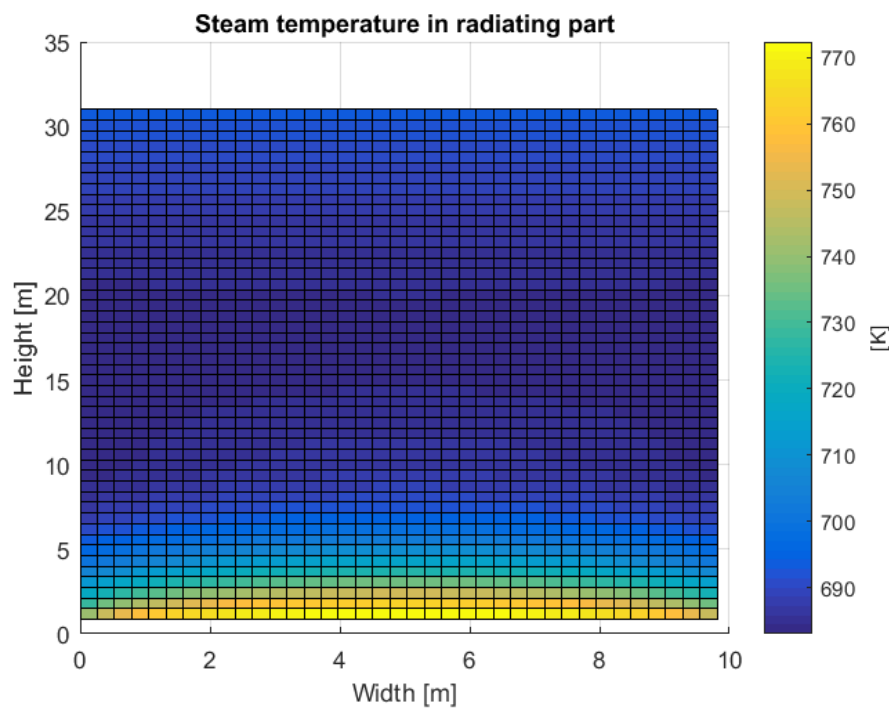


FIGURE 25: Temperature profile after 100 seconds.

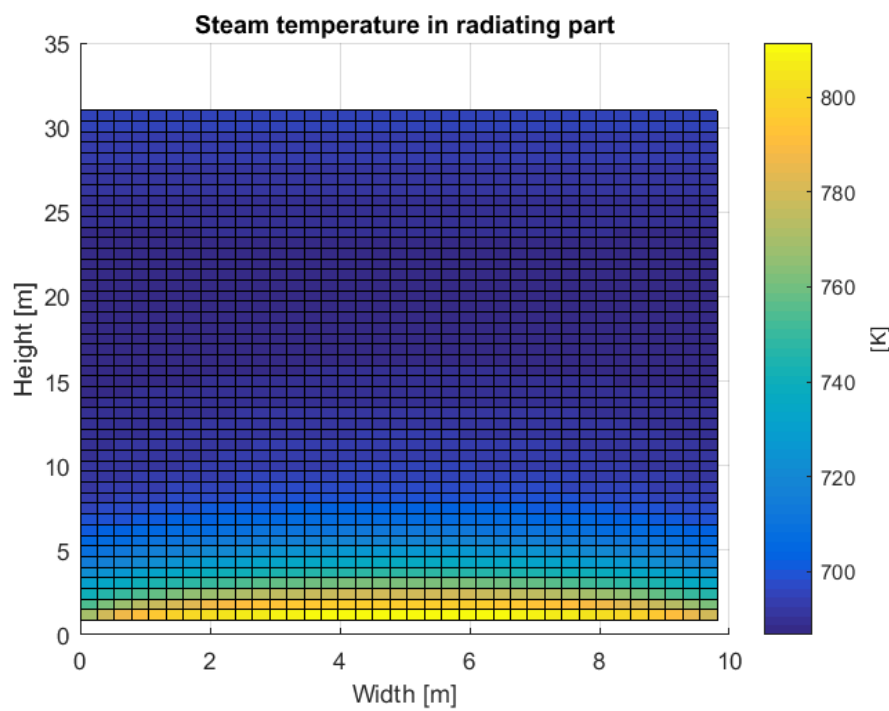


FIGURE 26: Temperature profile after 200 seconds.